Solid/Fluid Thermal Coupling Using the Immersed Boundary Method

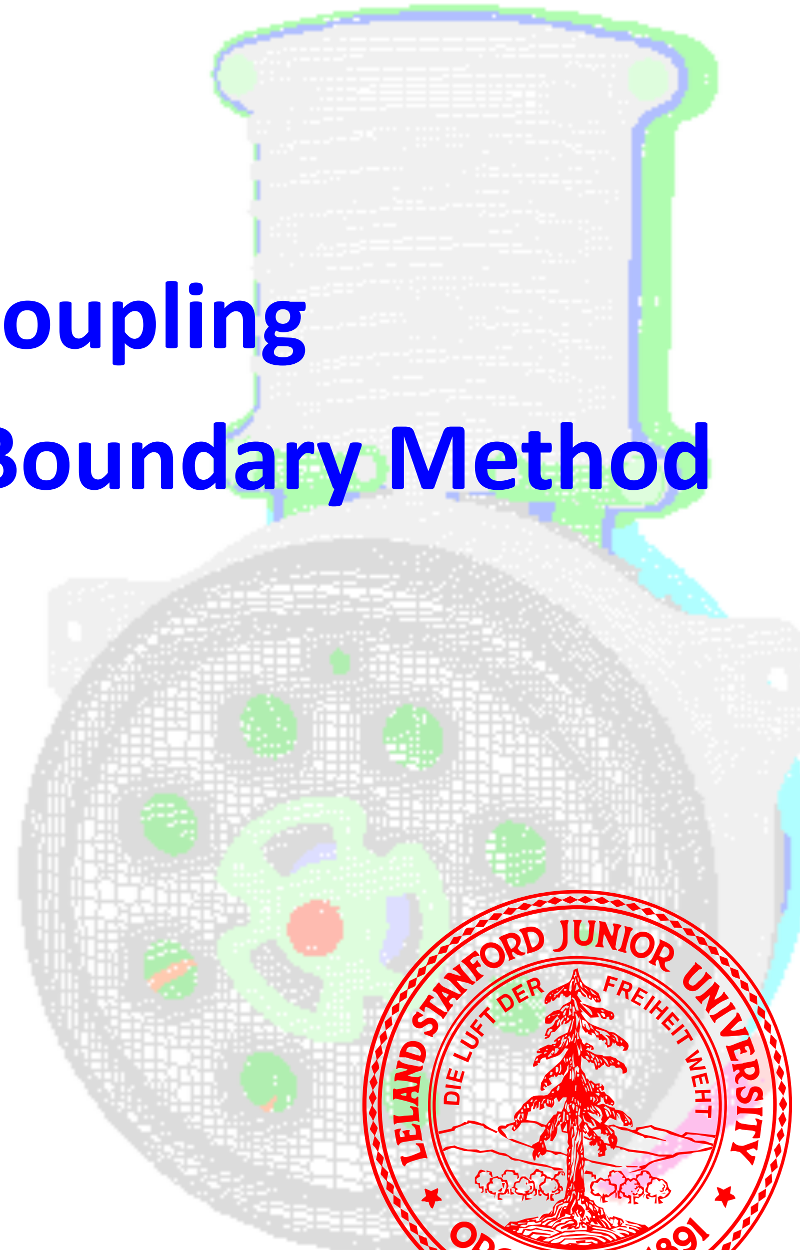

Gianluca Iaccarino
Mechanical Engineering
Stanford University

XXXV WSC Conference
October 6-10, 2010, Zeist, The Netherlands.

Non-Body-Fitted Approaches

- True Boundary

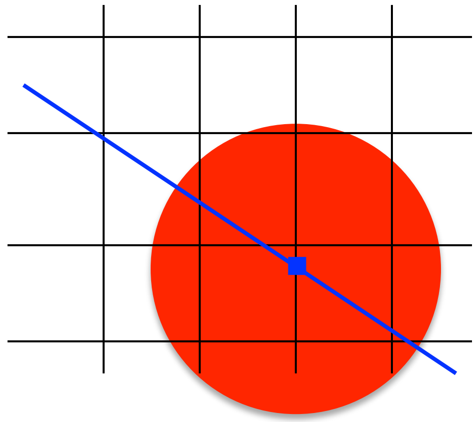

IB with Forcing

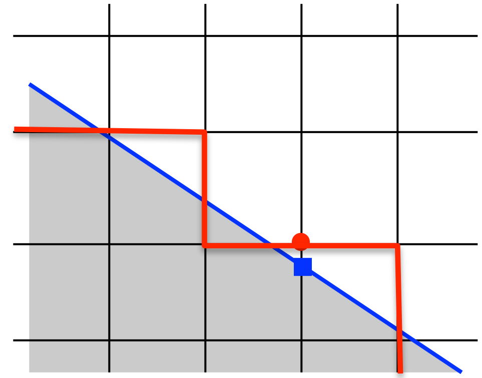

Stairstep/Mask

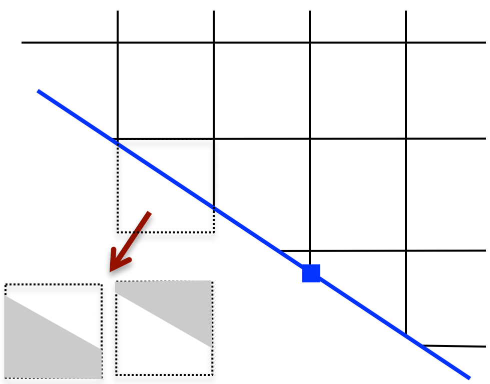

Cut-Cell (Body-Fitted)

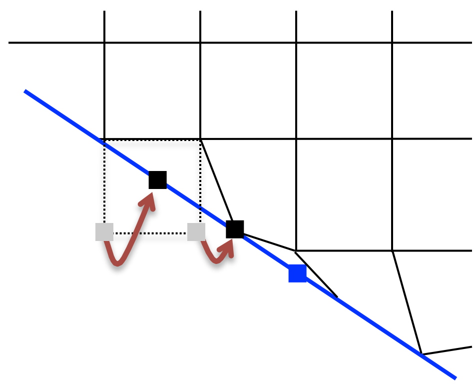

Projection (Body-Fitted)
OpenFoam SnappyHex

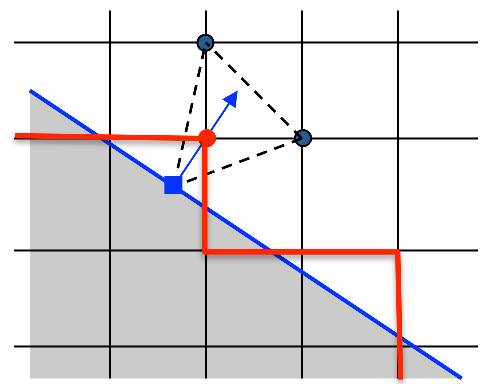

IB reconstruction

4. IB Reconstruction

Solid/Fluid Thermal Coupling
Using the Immersed Boundary Method

Geometric IB Reconstruction

Linear Reconstruction

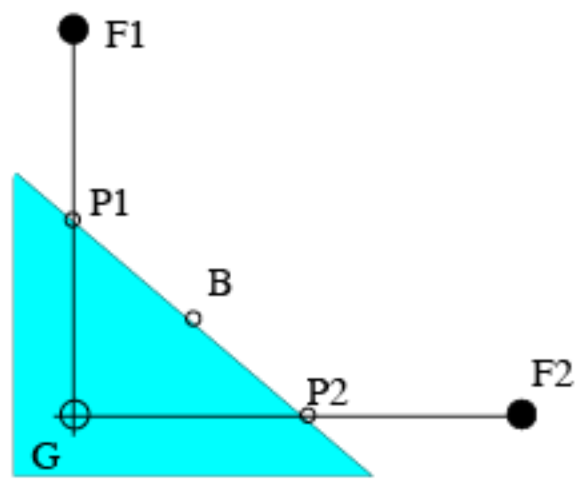

$$\phi = a_1 x + a_2 y + a_3$$

Quadratic Reconstruction

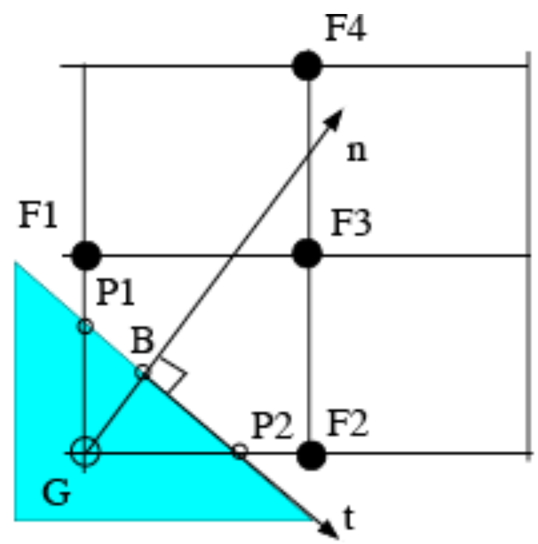

$$\phi = a_1 n^2 + a_2 n + a_3 t + a_4 nt + a_5$$

F: fluid points; B: boundary point; G: ghost point

Geometric IB Reconstruction

The quadratic reconstruction scheme requires 4 fluid nodes + BC

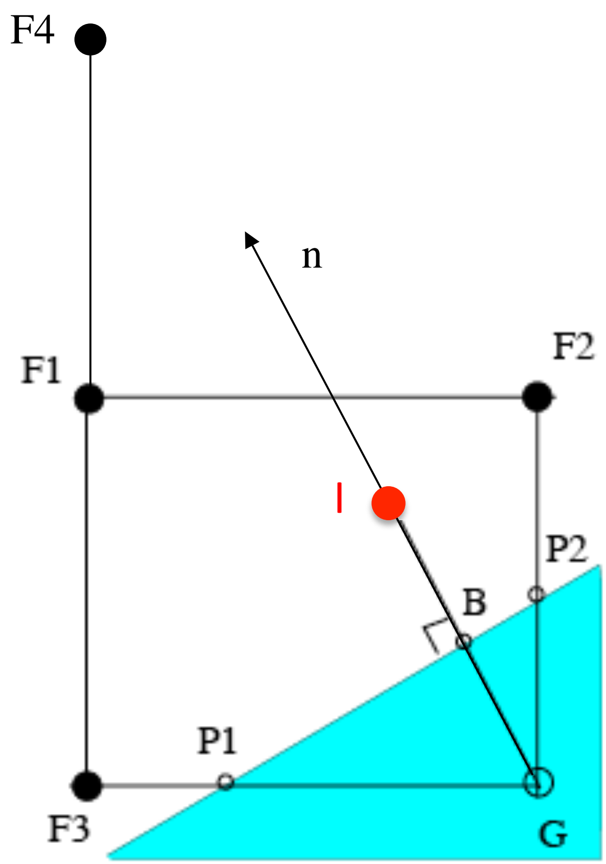

Remarks:

1) The fluid points F1-F4 are selected according to the angle between the IB and the grid
2) The image point is used to construct the interpolation and then the boundary value is reflected

F: fluid points; B: boundary point;
G: ghost point; I: image of the ghost point

Physics-based IB Reconstruction

The quadratic reconstruction scheme requires 4 fluid nodes + BC

We can build a better reconstruction by using the conservation of momentum in a "ghost" control volume
(4 fluid nodes + BC + conservation of mass)

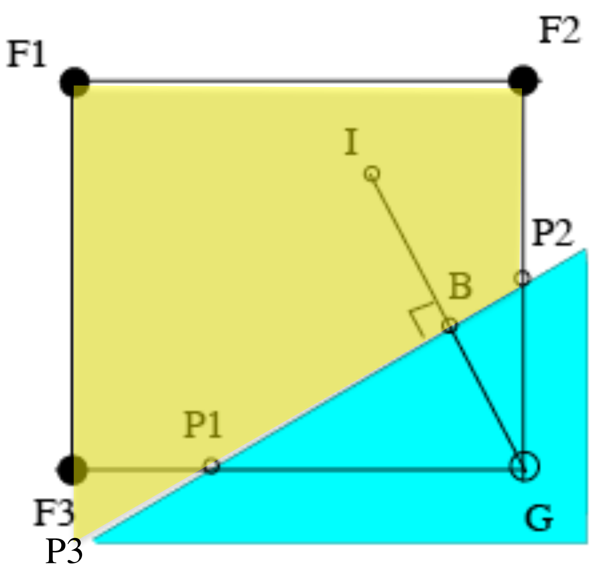

$$\phi = a_1 n^2 + a_2 n + a_3 t + a_4 nt + a_5$$

$$U\,(P2\text{-}F2) - U\,(P3\text{-}F1) + V\,(F1\text{-}F2) = 0$$

F: fluid points; B: boundary point;
G: ghost point; I: image of the ghost point
P: Additional surface points

Verification Test

Decaying vortex problem (exact solution of the Navier Stokes equations)

$$p(x,y,t) = -\frac{1}{4}(\cos 2\pi x + \cos 2\pi y)\, e^{-4\pi^2 t/\mathrm{Re}}$$

$$u(x,y,t) = -\cos\pi x \,\sin\pi y \; e^{-2\pi^2 t/\mathrm{Re}}$$

$$v(x,y,t) = \sin\pi x \,\cos\pi y \; e^{-2\pi^2 t/\mathrm{Re}}$$

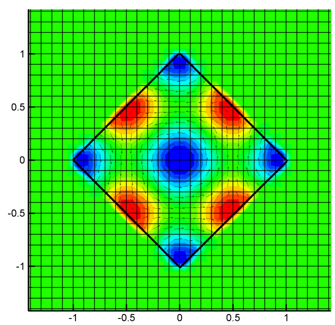

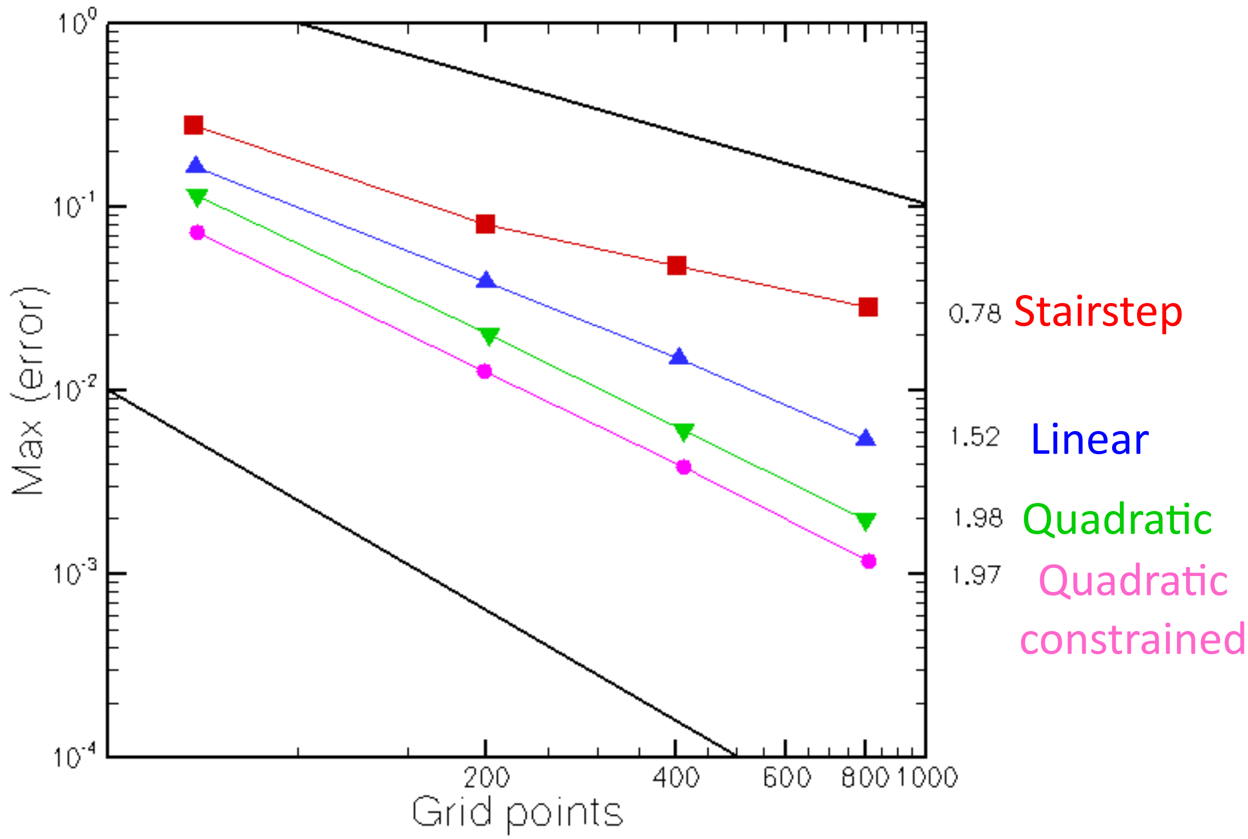

Achieved 2nd order accuracy at the Immersed Boundary

Reconstruction Schemes

- **Flow in an impeller stirred tank using an immersed boundary method.**
  R. Verzicco, G. Iaccarino, M. Fatica and P. Orlandi, CTR Annual Briefs ,2000
  1D linear, low-Re flow
- **RANS solver with adaptive structured boundary non-conforming grids**
  S. Majumdar, G. Iaccarino and P. Durbin, CTR Annual Briefs ,2001
  2D linear & quadratic, image point reflection, laminar flow
- **Turbulence modeling in an immersed-boundary RANS method**
  G. Kalitzin and G. Iaccarino, CTR Annual Briefs ,2002
  3D linear & inverse distance, turbulent flow, RANS
- **Wall modeling for large-eddy simulation using an immersed boundary method**
  F. Tessicini, G. Iaccarino, M. Fatica, M. Wang and R. Verzicco, CTR Annual Briefs , 2002
  3D linear/logarithmic, turbulent flow, LES
- **Accurate and efficient immersed-boundary interpolations for viscous flows**
  S. Kang, G. Iaccarino and P. Moin, CTR Annual Briefs, 2004
  3D linear & quadratic, mass conservation constaint, turbulent flow, LES
- **Immersed boundary for compressible flow simulations on semi-structured meshes**
  M. de Tullio and G. Iaccarino, CTR Annual Briefs , 2005
  3D linear & quadratic, compressible, turbulent flow, RANS
- **Automatic mesh generation for LES in complex geometries**
  G. Iaccarino and F. Ham, CTR Annual Briefs , 2005
  3D linear, local and global mass conserving reconstructions, turbulent flow, LES

Mass Conservation

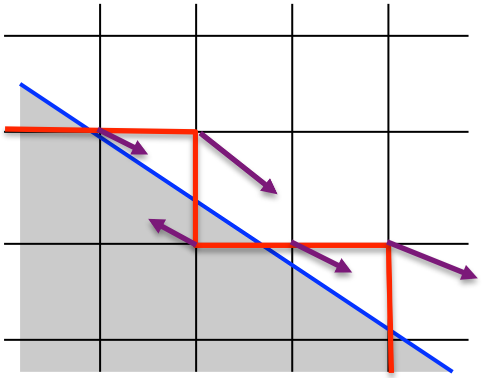

The Reconstructed stencils reflect the velocity at the ghost points…this can lead to large velocity divergence close to the boundary and pressure oscillations

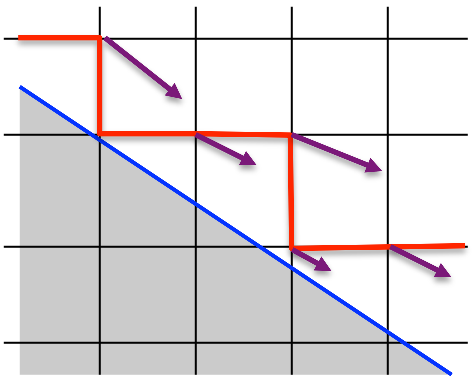

Forcing the IB "inside" the fluid domain eliminates the reflection!
However, The Reconstructed velocity at the virtual boundary still does not exactly conserve mass

$$\left(\vec{V}\cdot\hat{n}\right)_{IB} \neq 0$$ both locally and globally

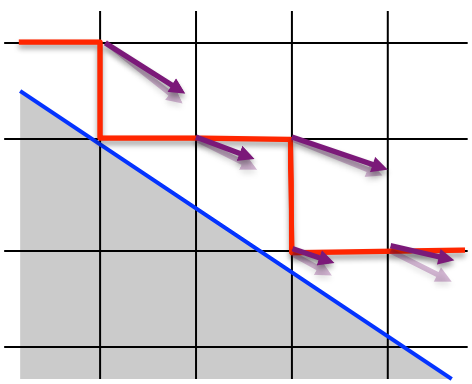

We can define a correction of the reconstruction based either on the global mass inbalance

$$\alpha\sum\left(\vec{V}\cdot\hat{n}\right)_{IB} A_{IB}$$ equally distributed at the IB nodes

or the local mass flux $\left(\vec{V}\cdot\hat{n}\right)_{IB}$

Laminar Channel

Use Cartesian grids generated in a rotated axis

- Periodic domain (no boundary conditions)
- Uniform grids (no effects of the numerical accuracy)

Test accuracy, symmetry, convergence

Used α =20,10,-10 and three grid resolutions

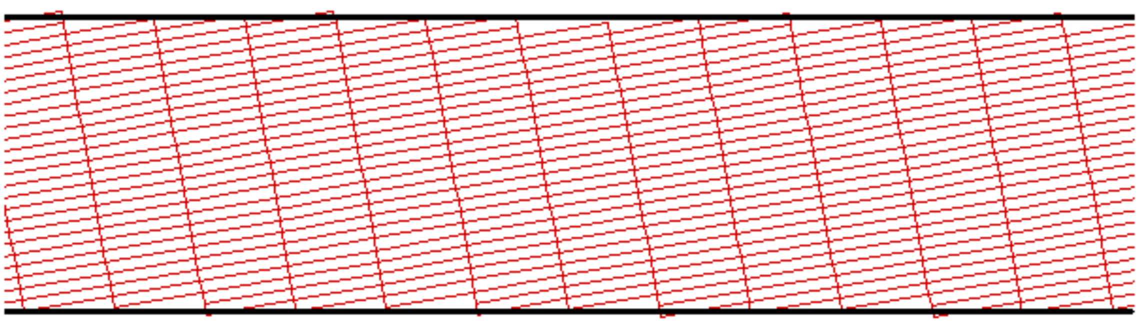

α = 10

StairStep Solution

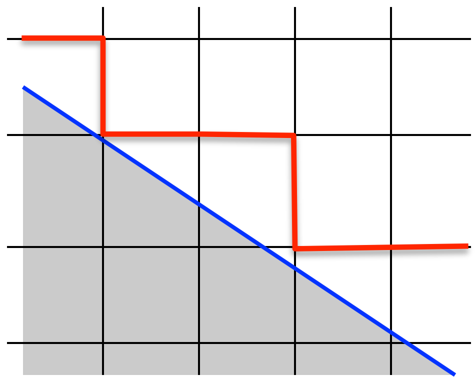

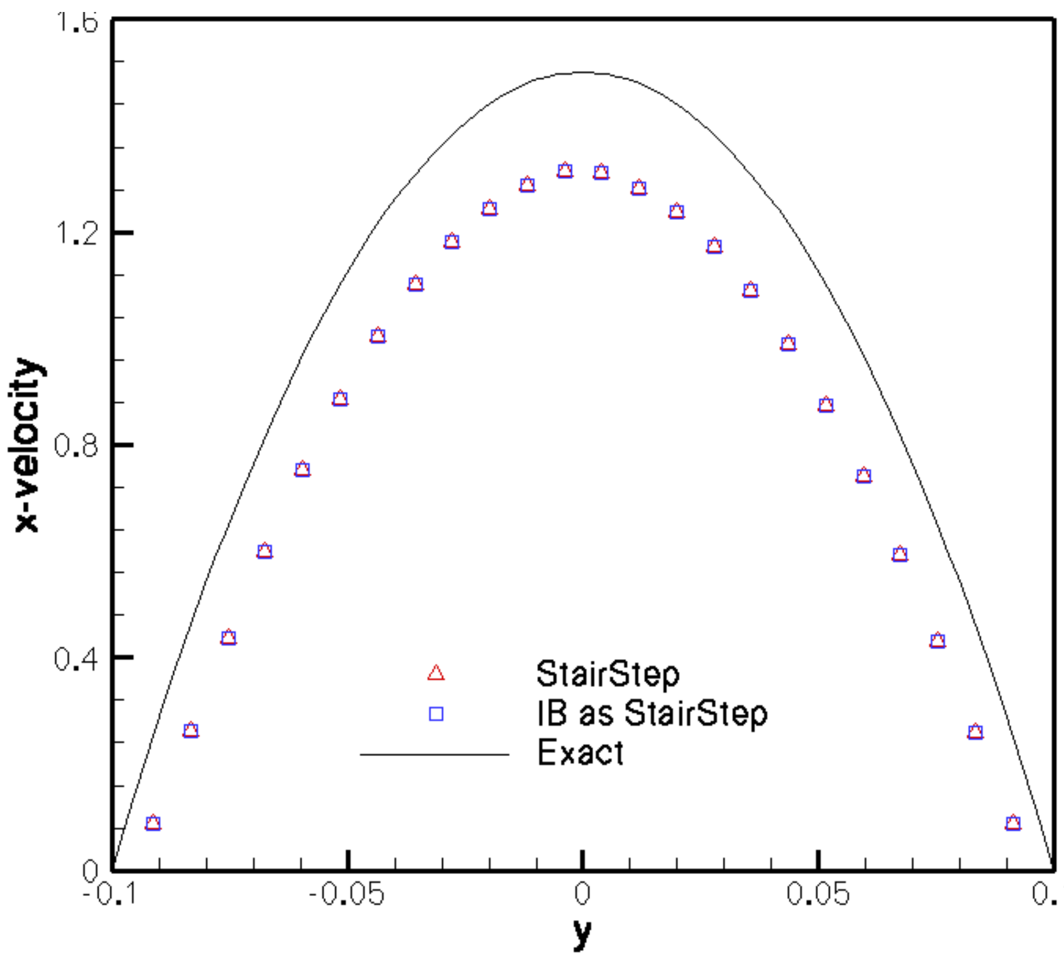

Remark: ibwalls are always inside the computational domain, hence we always obtain lower mass through (fixed pressure gradient!)

Mass Conservation

Effect of the mass correction applied to the ibwall interpolation

(Quadratic reconstruction)

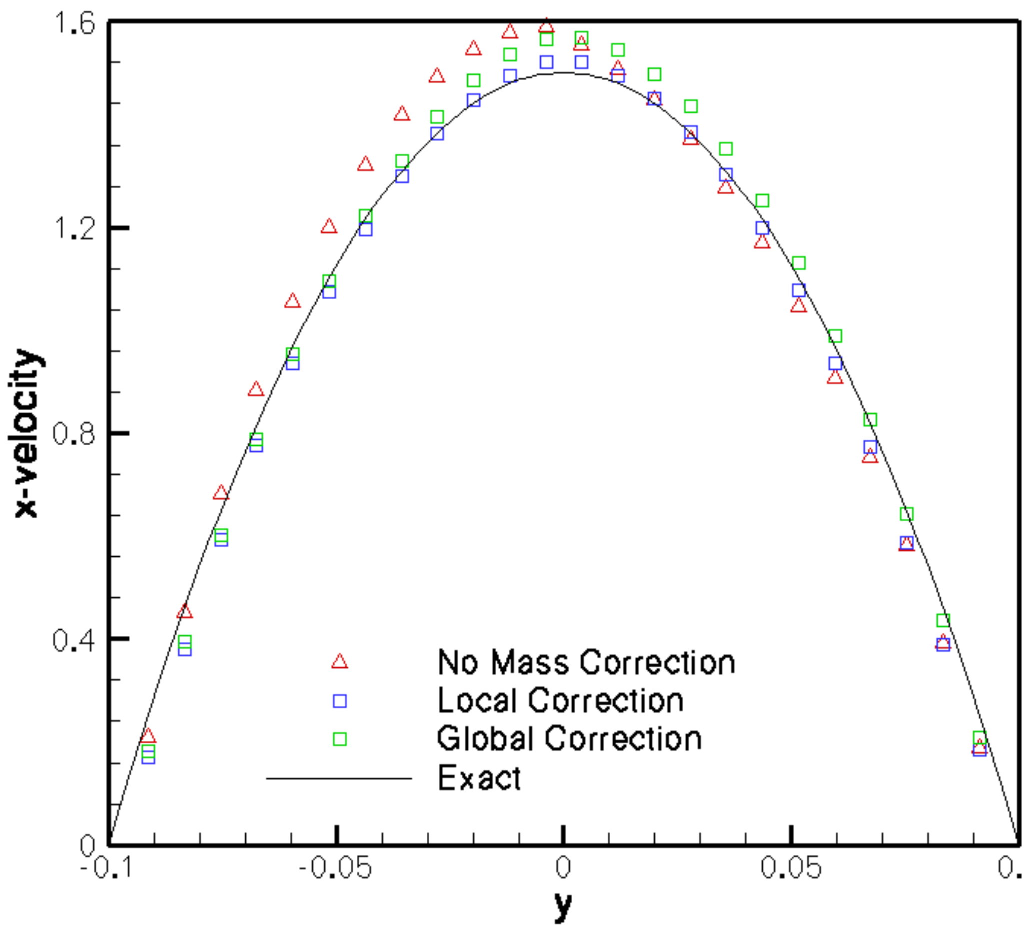

Remark: the asymmetry is related to the grid not being top/bottom symmetric. The corrections eliminate it almost completely!

Grid Sensitivity

The solution correctly converges independently of the mass correction used.

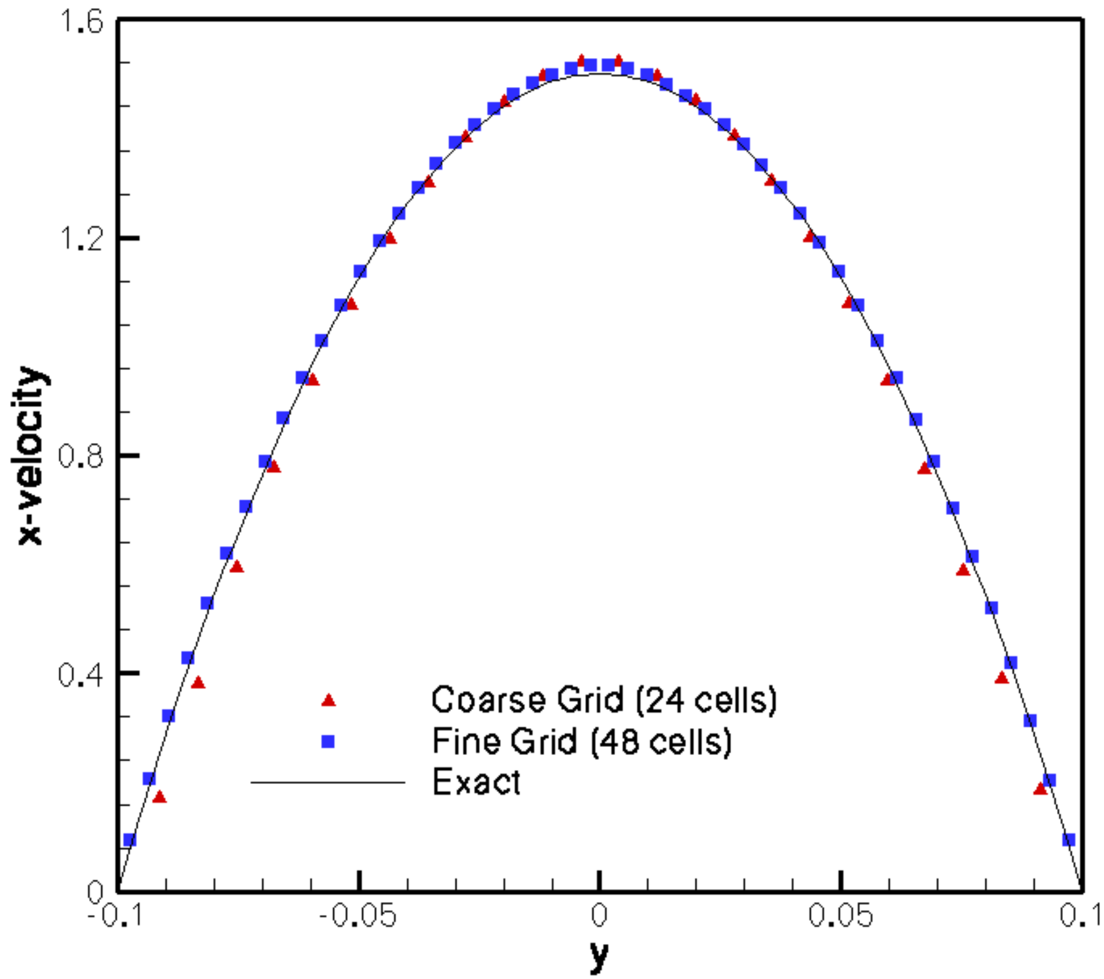

Grid Angle Sensitivity

Local mass correction provides a symmetric profile independently of the angle

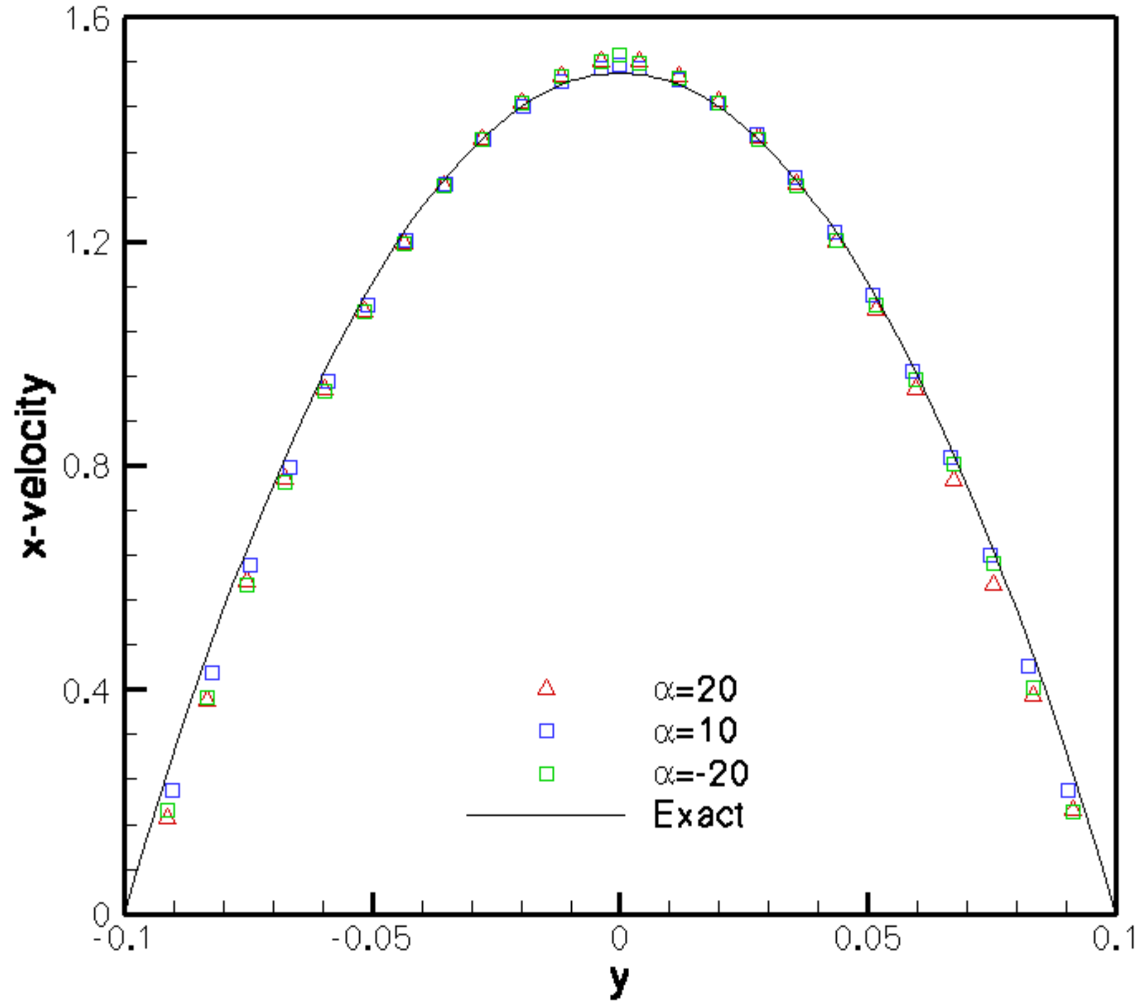

Verification Test

L^{∞} error in velocity

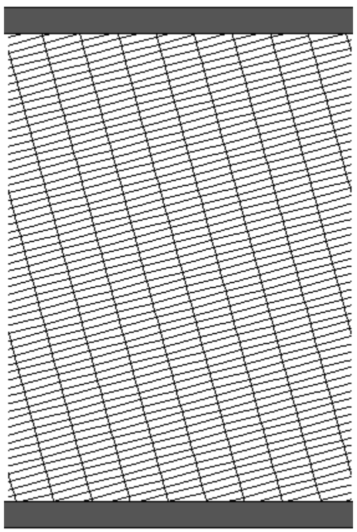

$\alpha = 15^{o}$

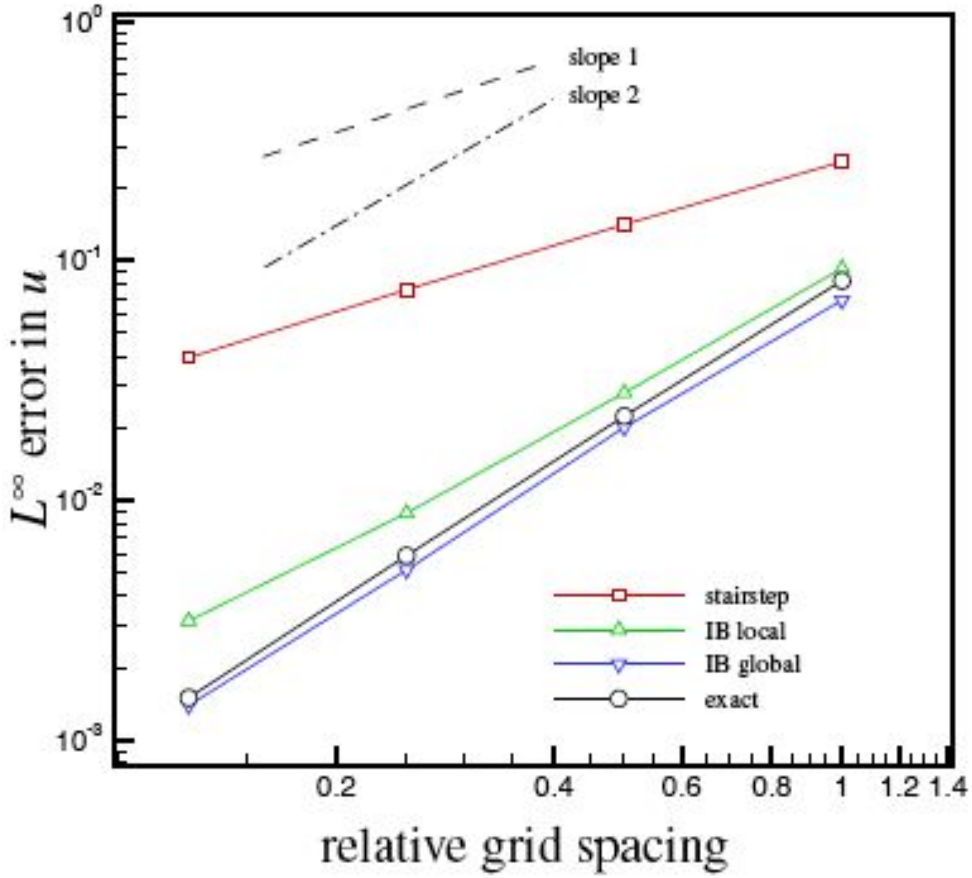

Numerical Method - Details

Navier-Stokes Equations – Incompressible Fluid

$$\frac{\partial u_i}{\partial t} + \frac{\partial u_i u_j}{\partial x_j} = -\frac{\partial p}{\partial x_i} + \frac{1}{Re}\frac{\partial^2 u_i}{\partial x_j \partial x_j}$$ Momentum

$$\frac{\partial u_i}{\partial x_i} = 0$$ Continuity

Fractional Step Method – Crank-Nicholson in time, RK for Convective Terms

$$\left[\frac{1}{\Delta t} - \frac{(\alpha_k + \beta_k)}{2Re}\frac{\partial^2}{\partial x_j \partial x_j}\right]\hat{u}_i^k = \frac{u_i^{k-1}}{\Delta t} - (\alpha_k + \beta_k)\frac{\partial p^{k-1}}{\partial x_i} - \alpha_k\left(\frac{\partial u_i u_j}{\partial x_j}\right)^{k-1} - \beta_k\left(\frac{\partial u_i u_j}{\partial x_j}\right)^{k-2} + \frac{(\alpha_k + \beta_k)}{2Re}\left(\frac{\partial^2 u_i^{k-1}}{\partial x_j \partial x_j}\right)$$ Momentum Predictor

$$\frac{\partial^2 \phi}{\partial x_j \partial x_j} = \frac{1}{(\alpha_k + \beta_k)\Delta t}\frac{\partial \hat{u}_i^k}{\partial x_i}$$ Diverge-free Constraint

$$u_i^k = \hat{u}_i^k - (\alpha_k + \beta_k)\Delta t \frac{\partial \phi}{\partial x_i}$$ Momentum Corrector

$$p^k = p^{k-1} + \phi$$ Pressure update

IB Reconstruction

Linear	$u_{i,c}^k = \omega_{i,1} u_{i,1}^k + \omega_{i,2} u_{i,2}^k + \omega_{i,\text{IB}} u_{i,\text{IB}}^k$
Revised Linear	$u_{i,c}^k = \omega_{i,1} u_{i,1}^k + \omega_{i,2} u_{i,2}^k + \omega_{i,\text{IB}} u_{i,\text{IB}}^k$ $\Delta u_{i,c} = \omega_{i,1} \Delta u_{i,1} + \omega_{i,2} \Delta u_{i,2} + \omega_{i,\text{IB}} \Delta u_{i,\text{IB}}$ $\Delta u_{i,c} = \hat{u}_{i,c}^k - u_{i,c}^{k-1}$
Quadratic	$\hat{u}_i^k(x_1, x_2) = a_{i,1}^k x_1^2 + b_{i,1}^k x_1 + a_{i,2}^k x_2^2 + b_{i,2}^k x_2 + \hat{u}_{i,c}^k$
Quadratic + Momentum	$\hat{u}_i^k(x_1, x_2) = a_{i,1}^k x_1^2 + b_{i,1}^k x_1 + a_{i,2}^k x_2^2 + b_{i,2}^k x_2 + \hat{u}_{i,c}^k$ $\frac{\hat{u}_{i,c}^k}{\Delta t} - \frac{(\alpha_k + \beta_k)}{Re}(a_{i,1}^k + a_{i,2}^k) = \frac{u_{i,c}^{k-1}}{\Delta t} - (\alpha_k + \beta_k)\frac{\partial p^{k-1}}{\partial x_i} - \alpha_k \left(\frac{\partial u_i u_j}{\partial x_j}\right)^{k-1} - \beta_k \left(\frac{\partial u_i u_j}{\partial x_j}\right)^{k-2} + \frac{(\alpha_k + \beta_k)}{2Re}\frac{\partial^2 u_i^{k-1}}{\partial x_j \partial x_j}$

IB Reconstruction

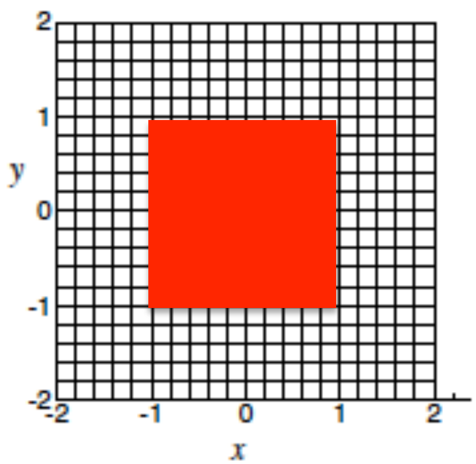

Decaying Taylor Vortices

Exact Solution of NS Eqs.

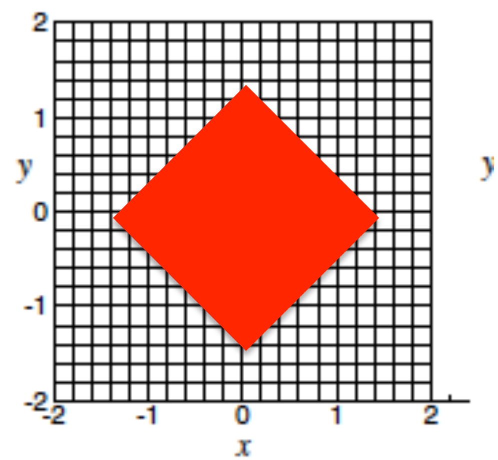

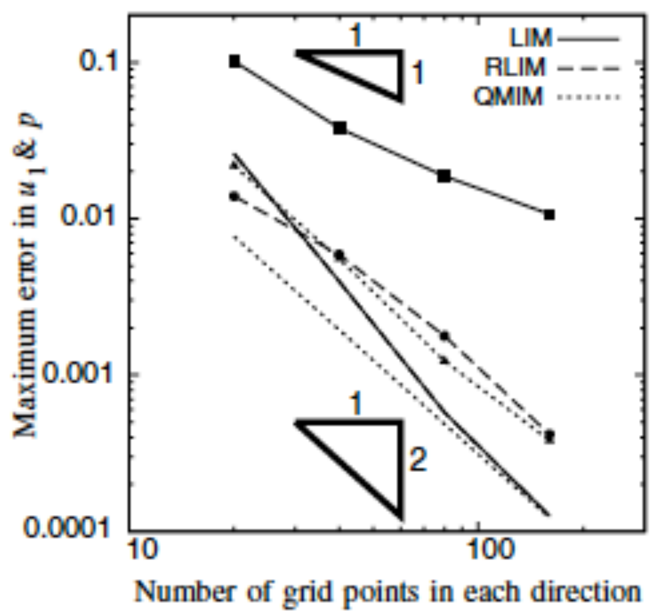

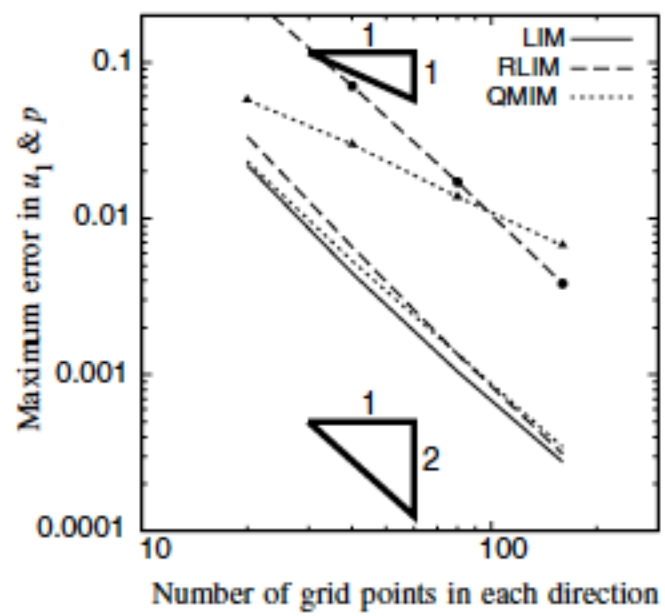

LES of airfoil flow

Re ~ 150,000 - Grid size ~7M

- Local mesh refinement technique reduces the total number of mesh points by 70% compared to a (single-block) Cartesian mesh with similar mesh resolution near the wall

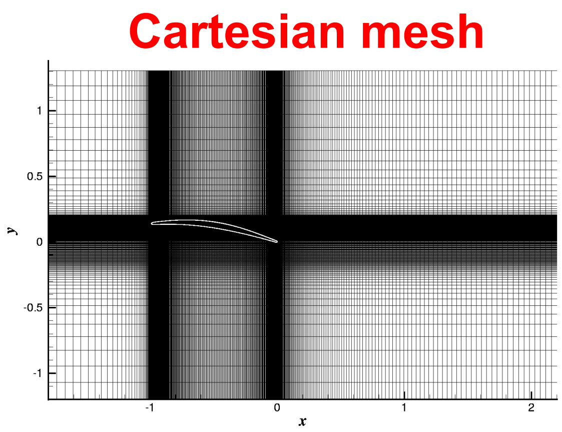

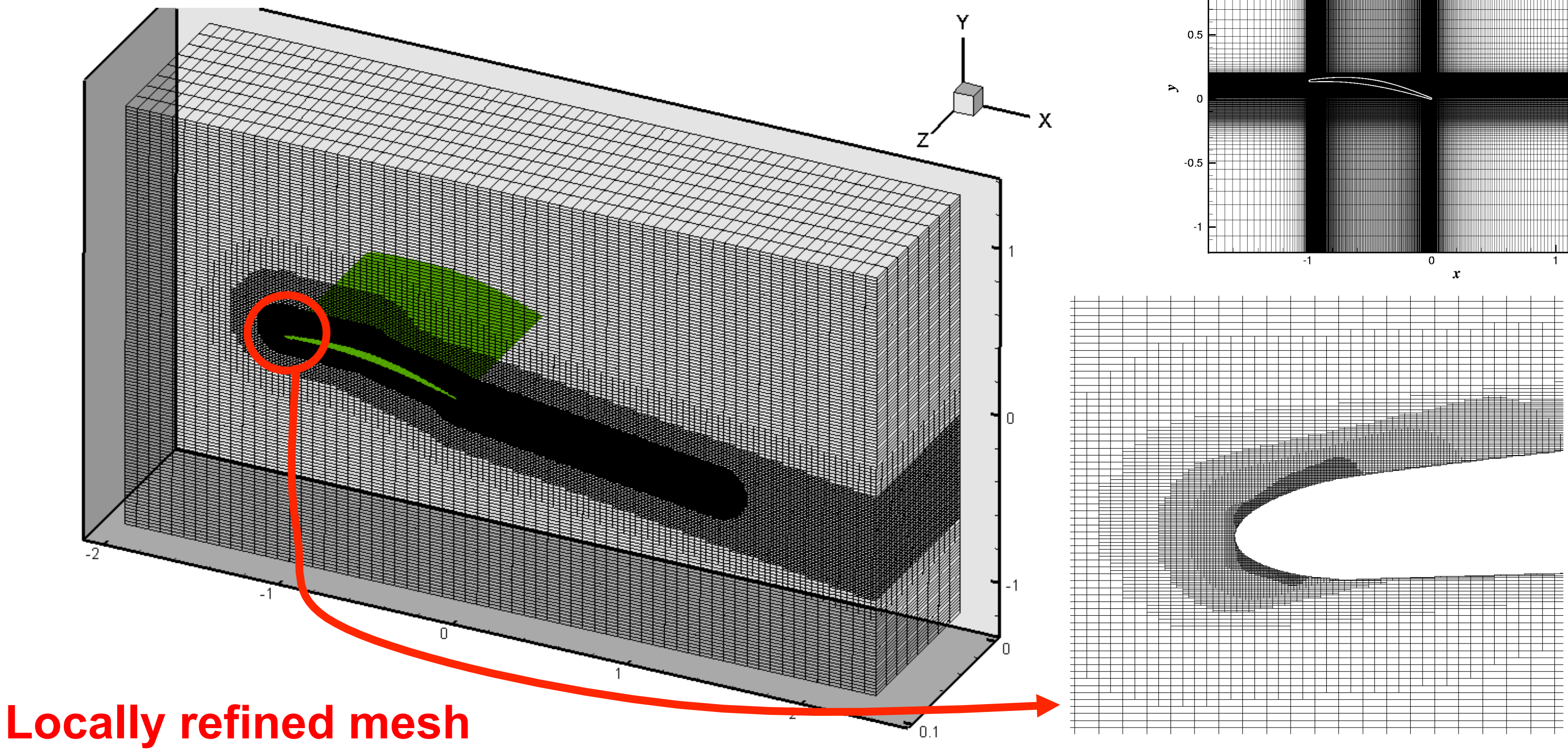

LES of airfoil flow

Re ~ 150,000 - Grid size ~7M

Small separation bubble near LE prompts transition to turbulence

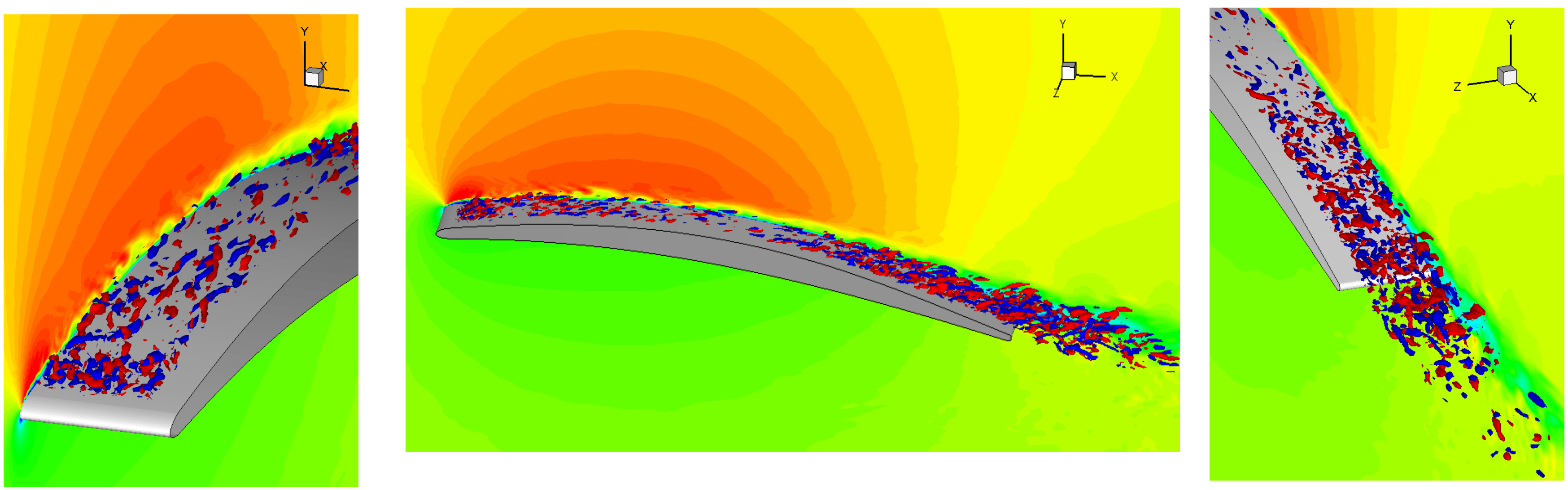

Instantaneous *x*-velocity and *x*-vorticity

LES of airfoil flow

Re ~ 150,000 - Grid size ~7M

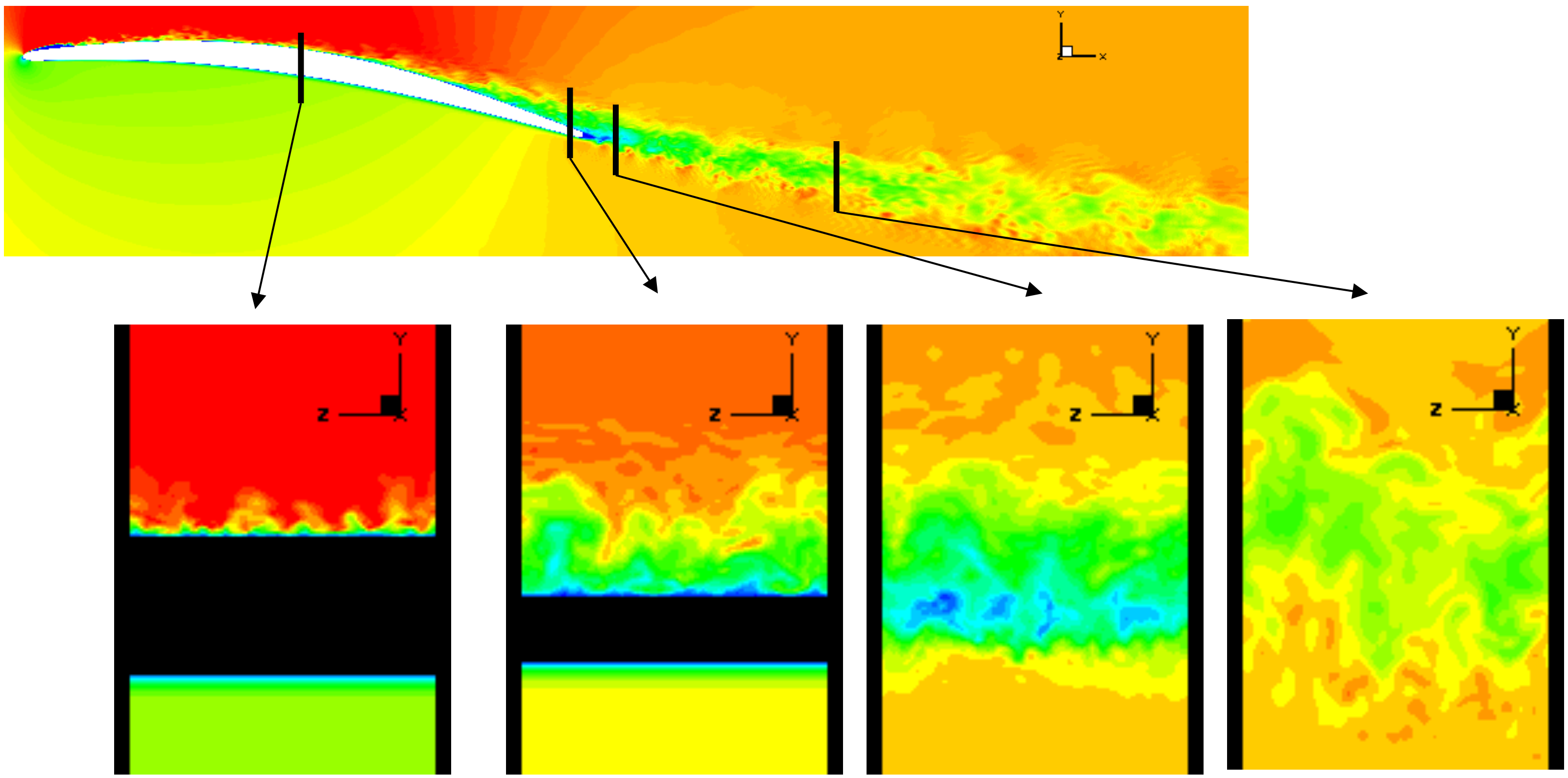

Streamwise velocity

Mean Flow Predictions

Over the airfoil

Downstream

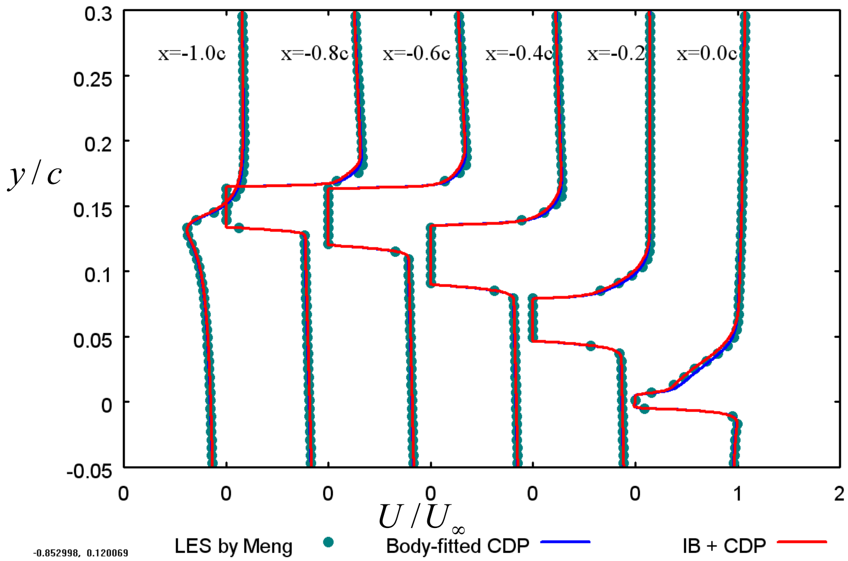

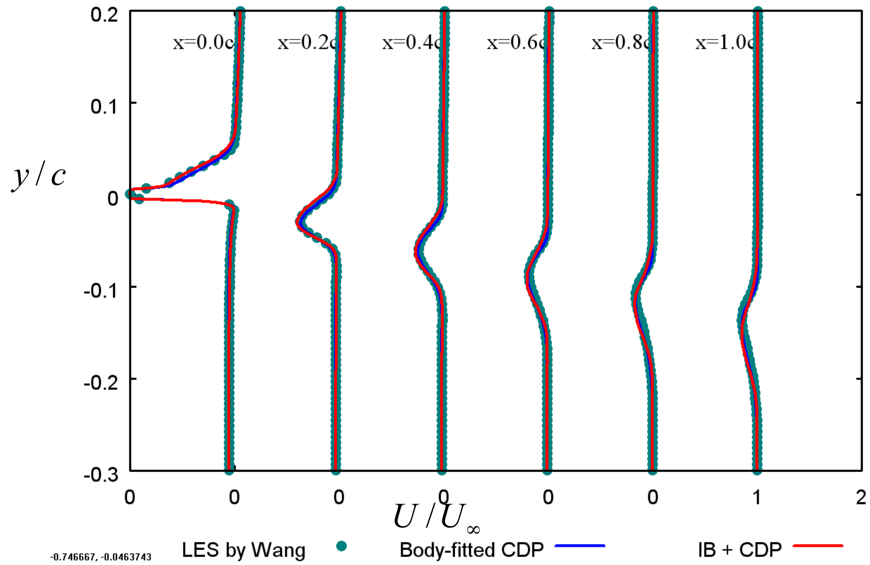

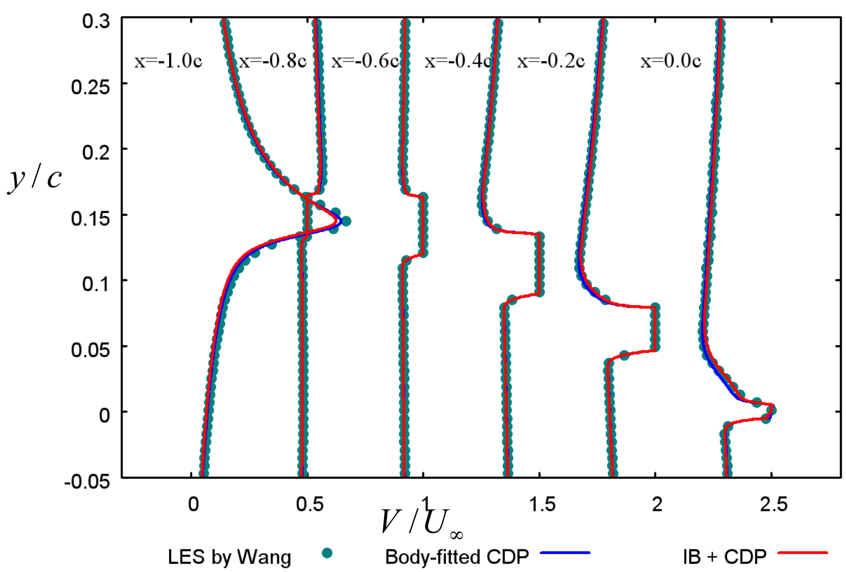

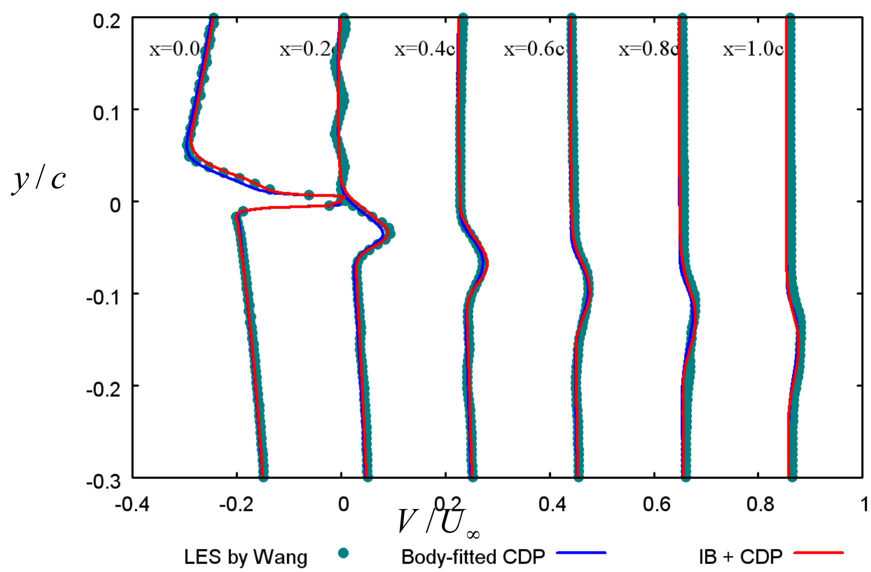

Acoustic Predictions

Comparisons of velocity profiles in the wake and pressure distribution on the surface is very favorable

Much more challenging is the prediction of the wall pressure fluctuations

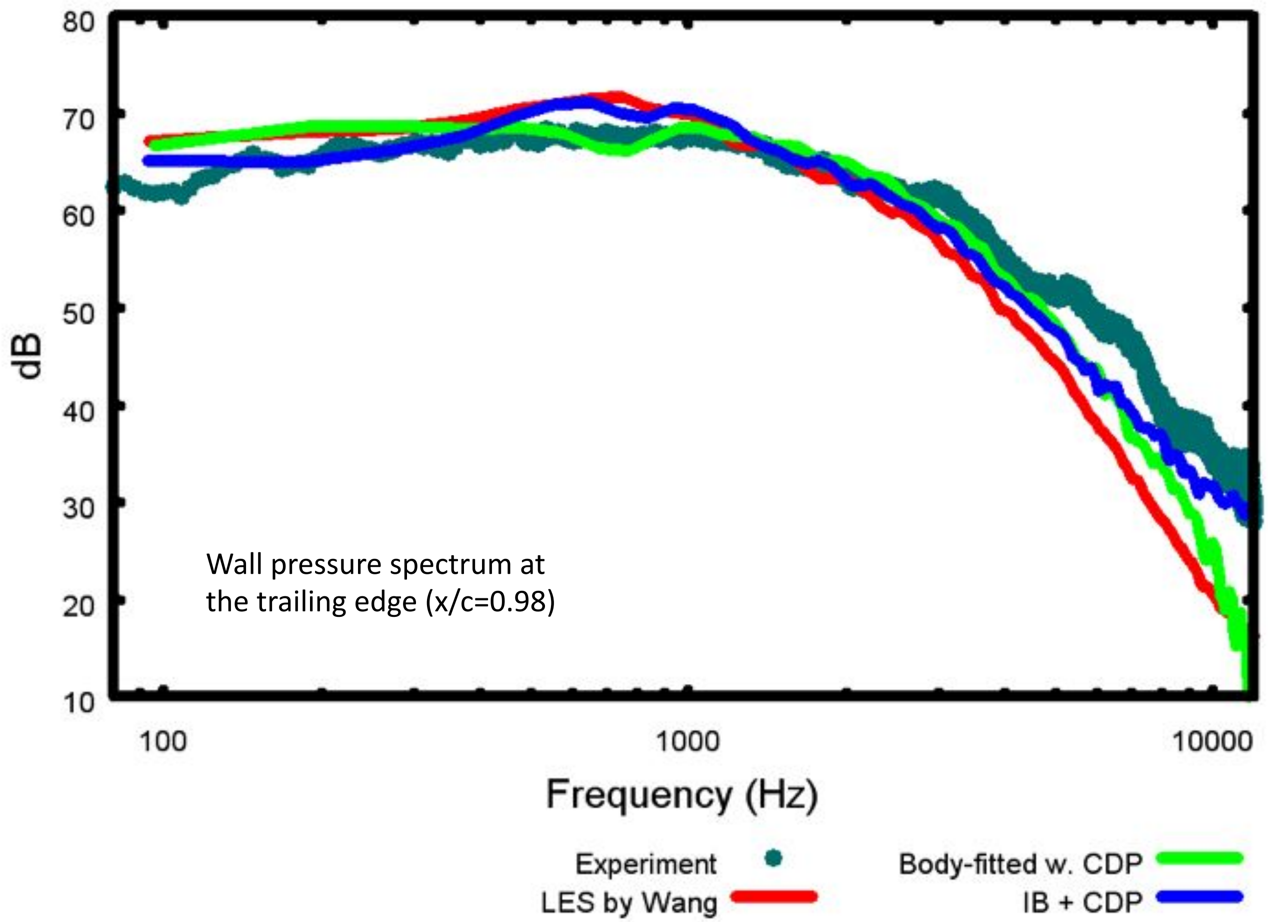

Summary

IB faces (ibwalls) are always inside the computational domain: effectively the reconstruction is always an interpolation

Use of Locally Refined Grid creates additional complexity in the reconstruction step

Enforcing mass conservation is NOT trivial but important and lead to more accurate results!

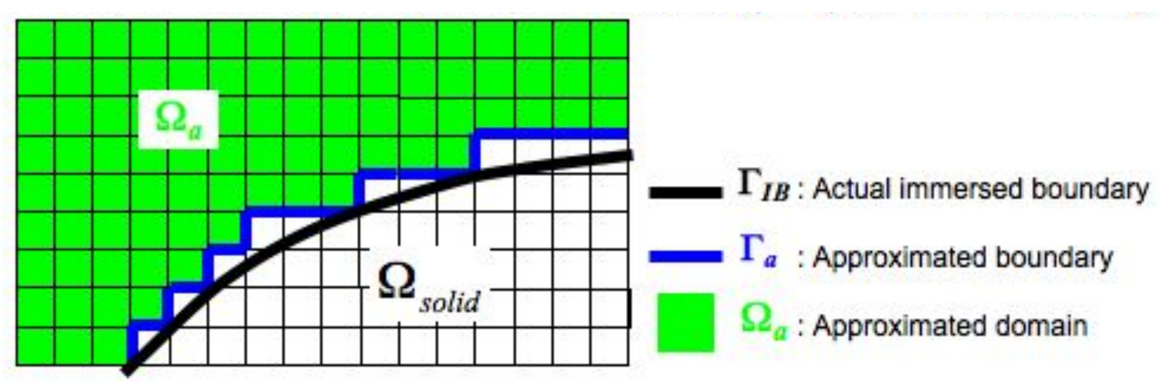

5. Solid/Fluid Thermal Coupling

Solid/Fluid Thermal Coupling
Using the Immersed Boundary Method

Multi-Domain Coupling

Fluid

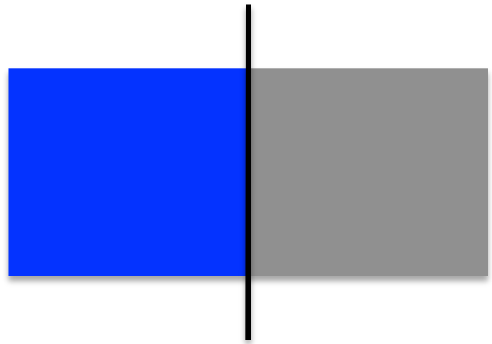

Solid

$$\frac{\partial \rho h}{\partial t} + \frac{\partial \rho u_j h}{\partial x_j} = \frac{\partial}{\partial x_j}\left[k \frac{\partial T}{\partial x_j}\right]$$

Because of discontinuities in physical properties (conductivity, etc) it is preferred to apply boundary conditions rather than differentiate across the interface!

Multi-Domain Coupling

Fluid

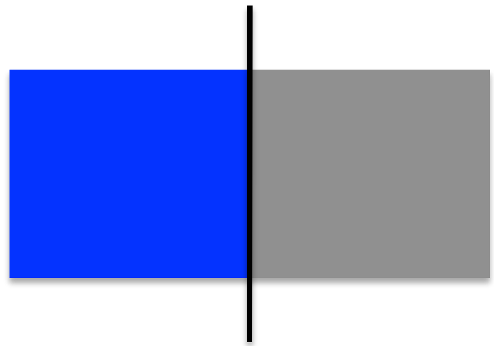

Solid

Interface Conditions

$$
\begin{cases}
T_{fluid} = T_{solid} \\
k_{solid} \left.\dfrac{\partial T}{\partial n}\right|_{solid} = k_{fluid} \left.\dfrac{\partial T}{\partial n}\right|_{fluid}
\end{cases}
$$

Multi-Domain Coupling

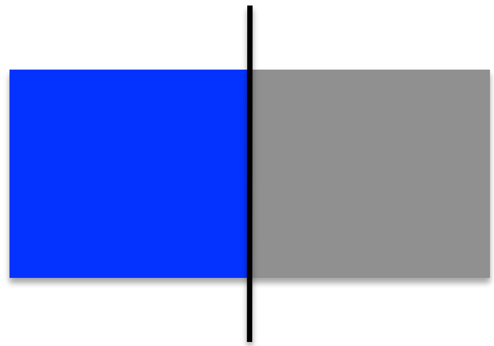

Fluid

Solid

Coupling Relaxation Parameter

Interface Conditions

$$T_{fluid} = T_{solid}$$

$$k_{solid} \left.\frac{\partial T}{\partial n}\right|_{solid} = k_{fluid} \left.\frac{\partial T}{\partial n}\right|_{fluid} + \eta \times \left(T_{solid} - T_{fluid}\right)$$

Multi-Domain Coupling

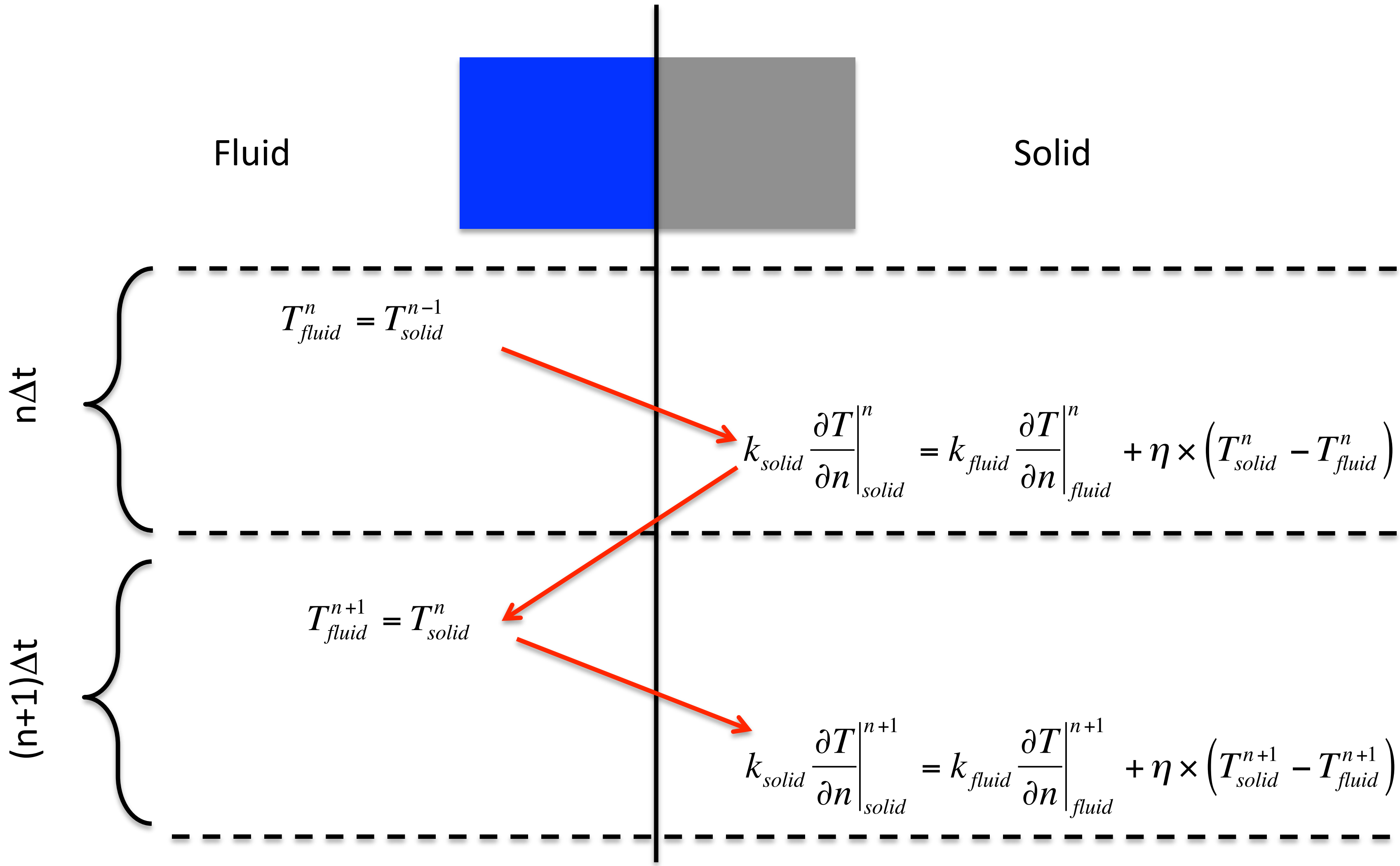

Staggered coupling procedure

IB Multi-Domain Coupling

The energy equation is NOT solved across the subdomains, but boundary conditions are formally applied at the interface

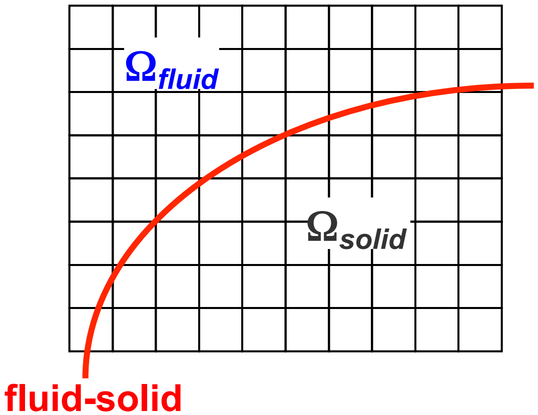

true domain boundary

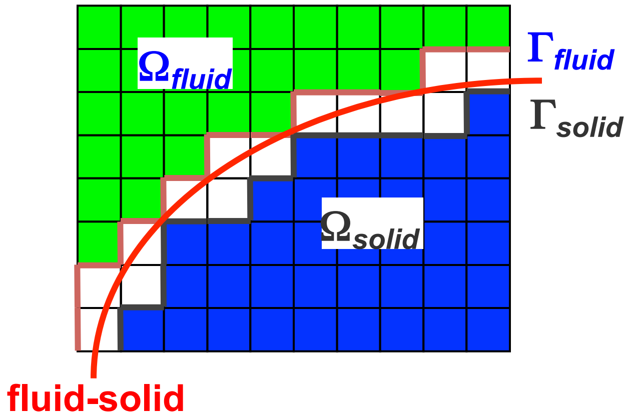

approximated domain boundary

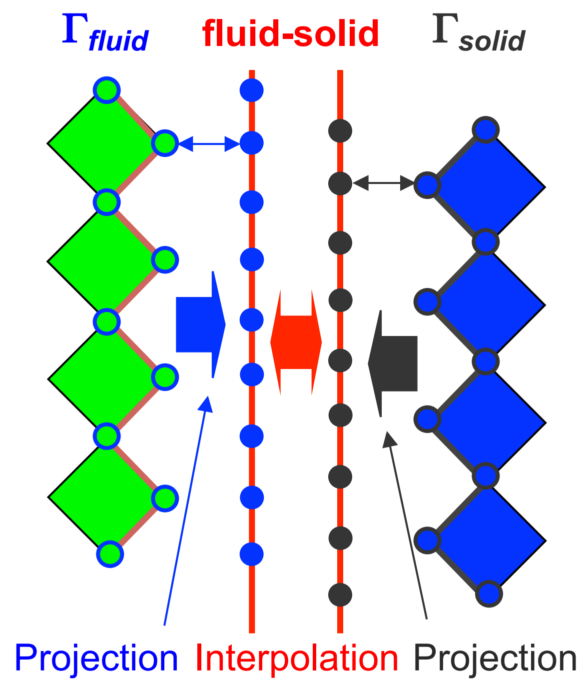

coupling condition

We apply the IB reconstruction method on both sides of the interface

IB Multi-Domain Coupling

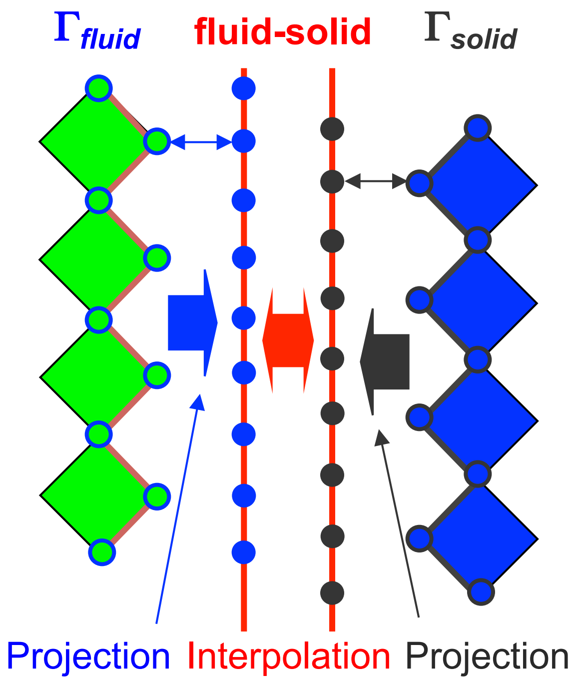

What is actually coupled?

Continuity of temperature

$$T_{fluid} = \overline{T_{solid}}$$

Continuity of heat flux

$$k_{solid} \left. \frac{\partial T}{\partial n} \right|_{solid} = \overline{k_{fluid} \left. \frac{\partial T}{\partial n} \right|_{fluid}}$$

Overbar indicates surface interpolation operators (on the "true" surface)

Asymmetric boundary condition enforcement

Interface Interpolation

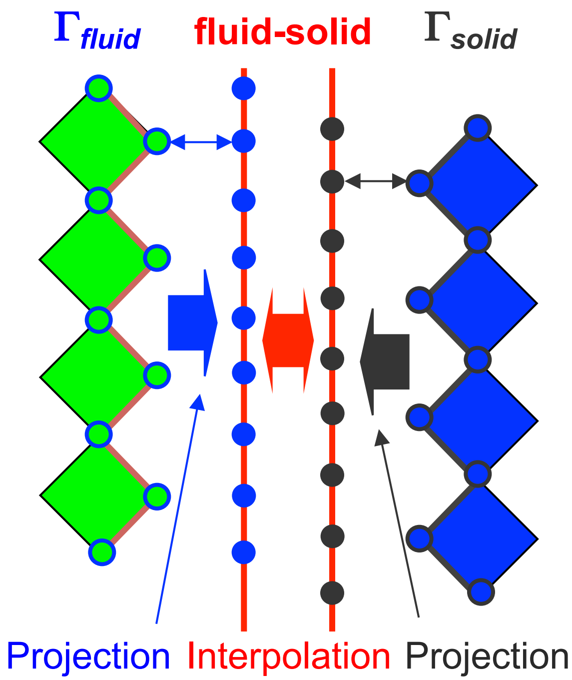

We need the actual interface geometry….

Interface Grid Reconstruction

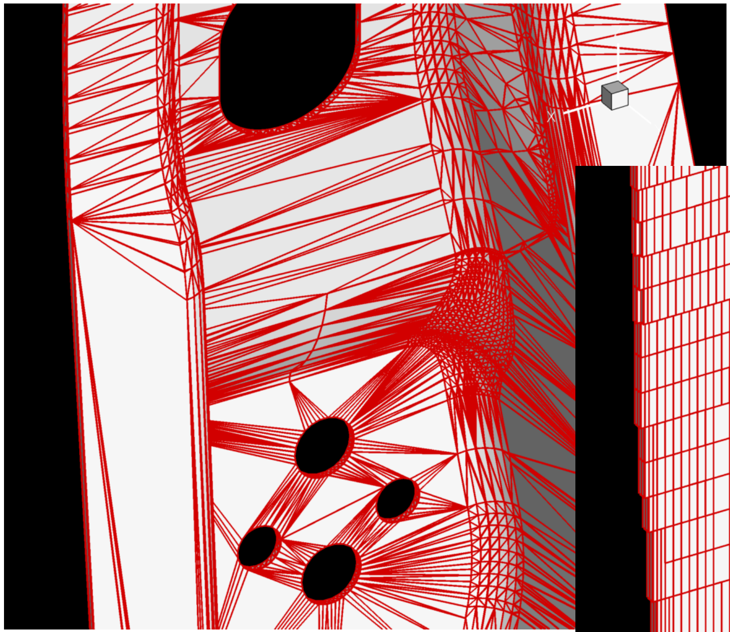

original stl

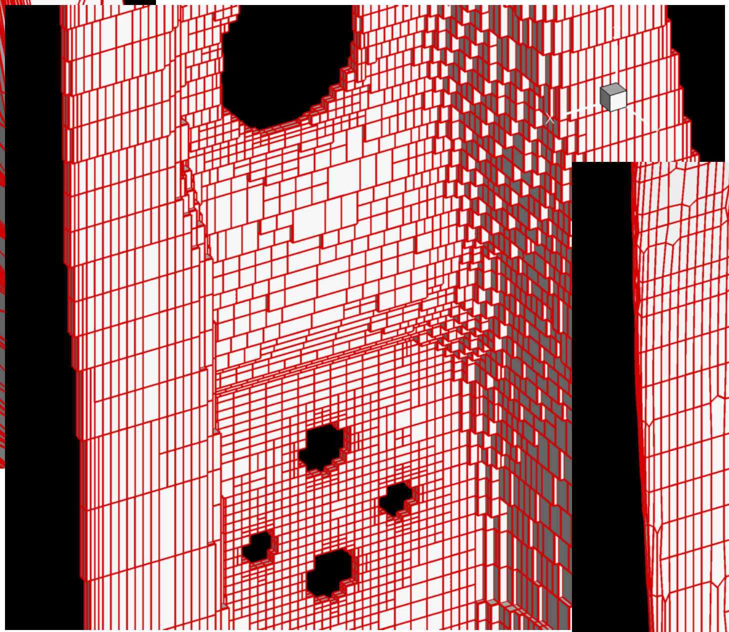

stairstep tommie grid

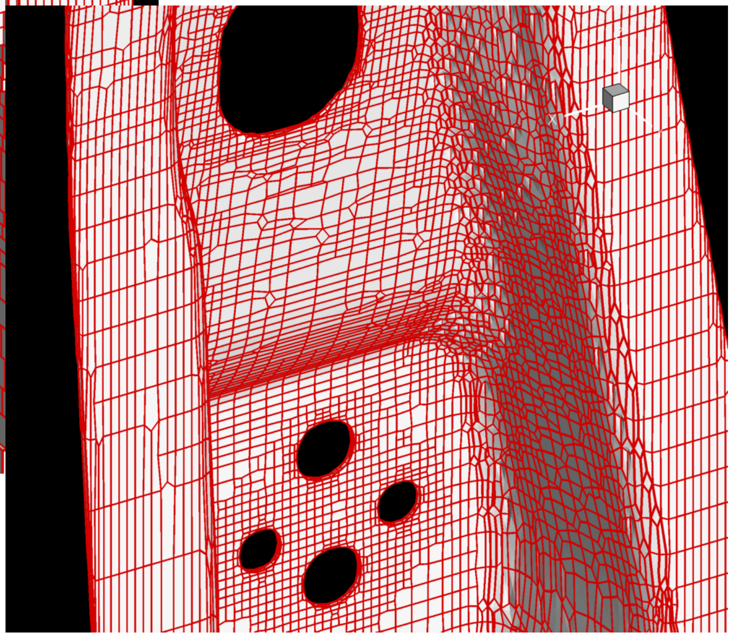

projected tommie grid

Interface Interpolation

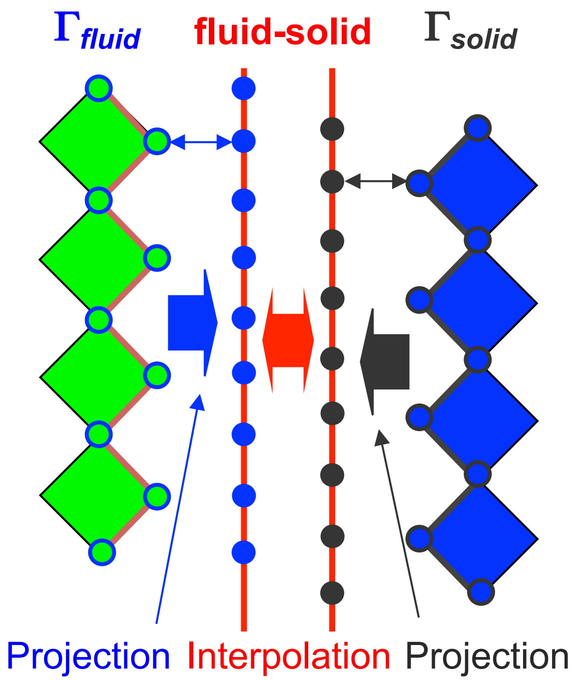

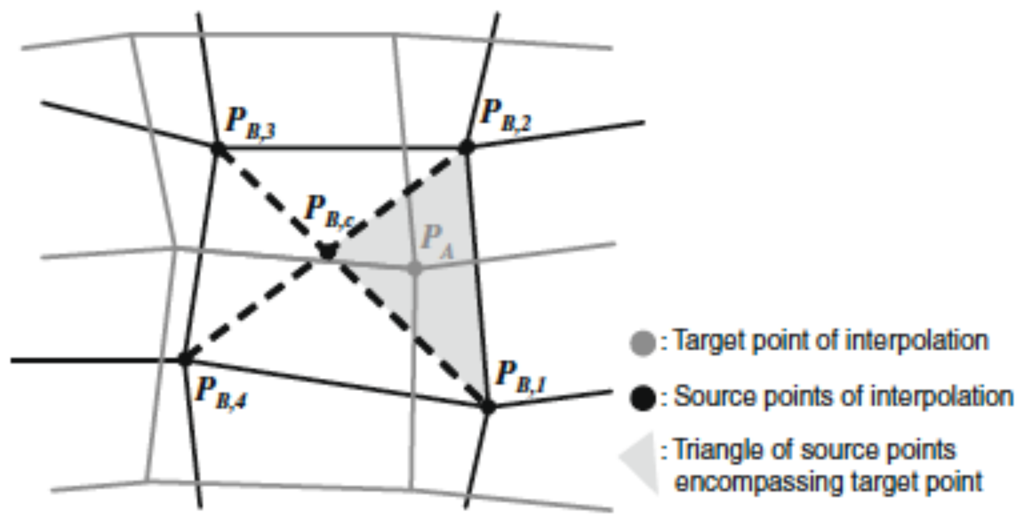

Validation Test, I

Flow generated by a heated sphere
$Gr = 10^4$
Constant temperature on the sphere
Natural convection, Boussinesq approximation

Mesh:
~2.2M elements

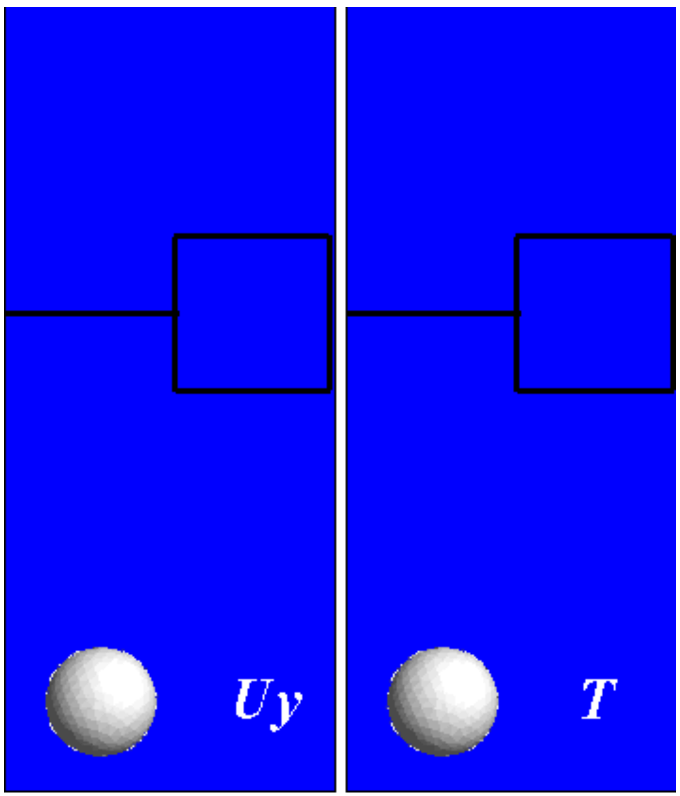

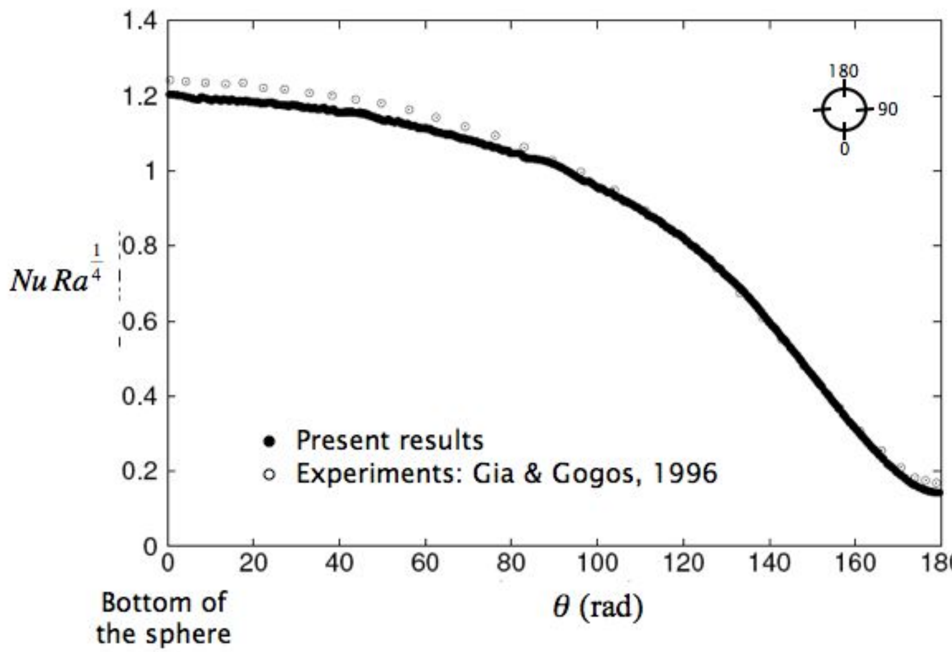

Validation Test, II

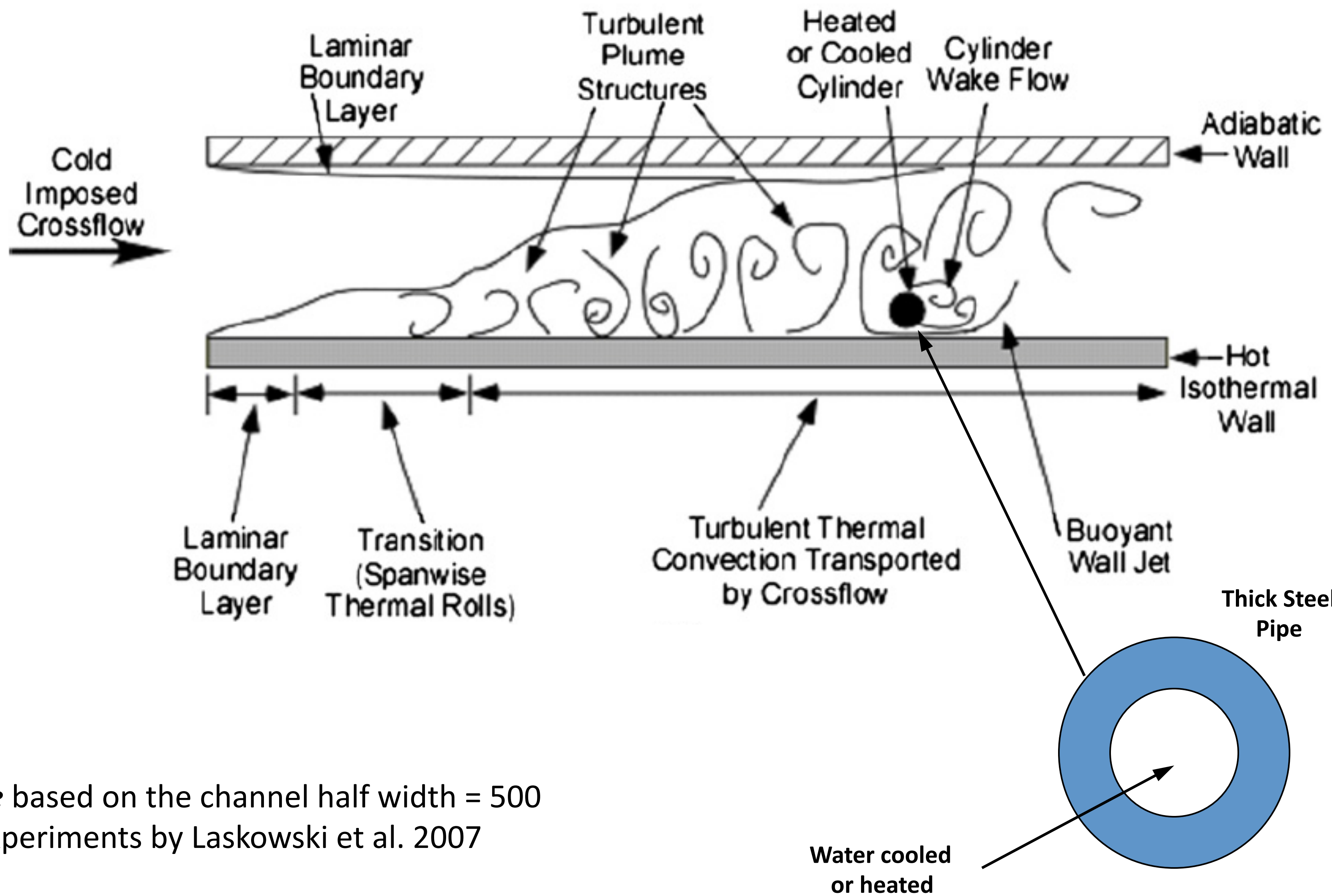

Re based on the channel half width = 500
Experiments by Laskowski et al. 2007

Computational Mesh

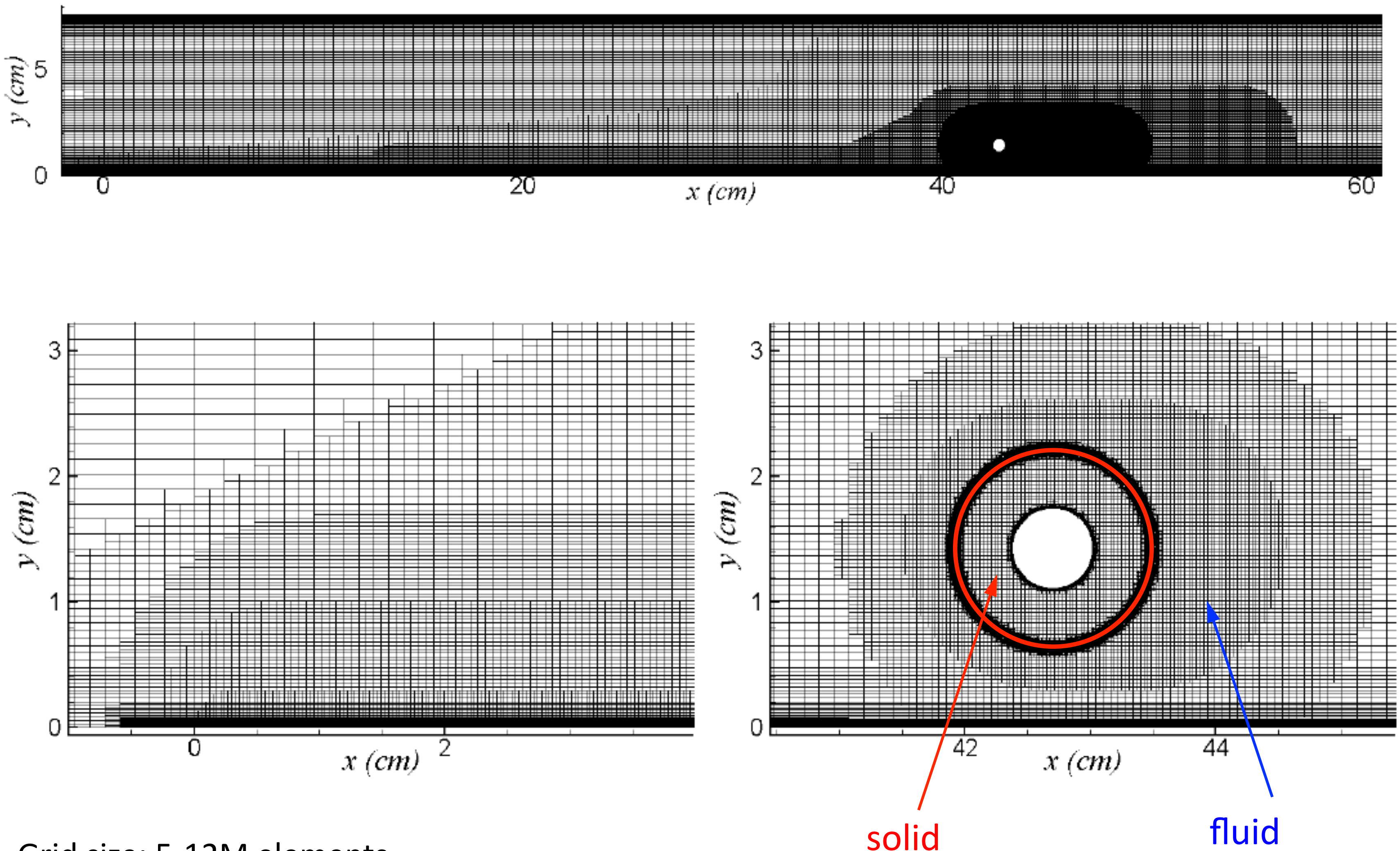

Grid size: 5-12M elements

Simulation Results

Temperature field

Side view

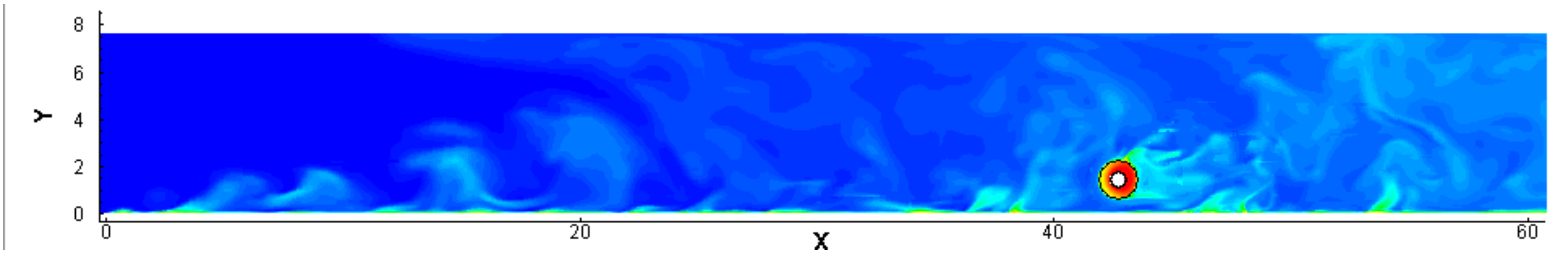

Top view

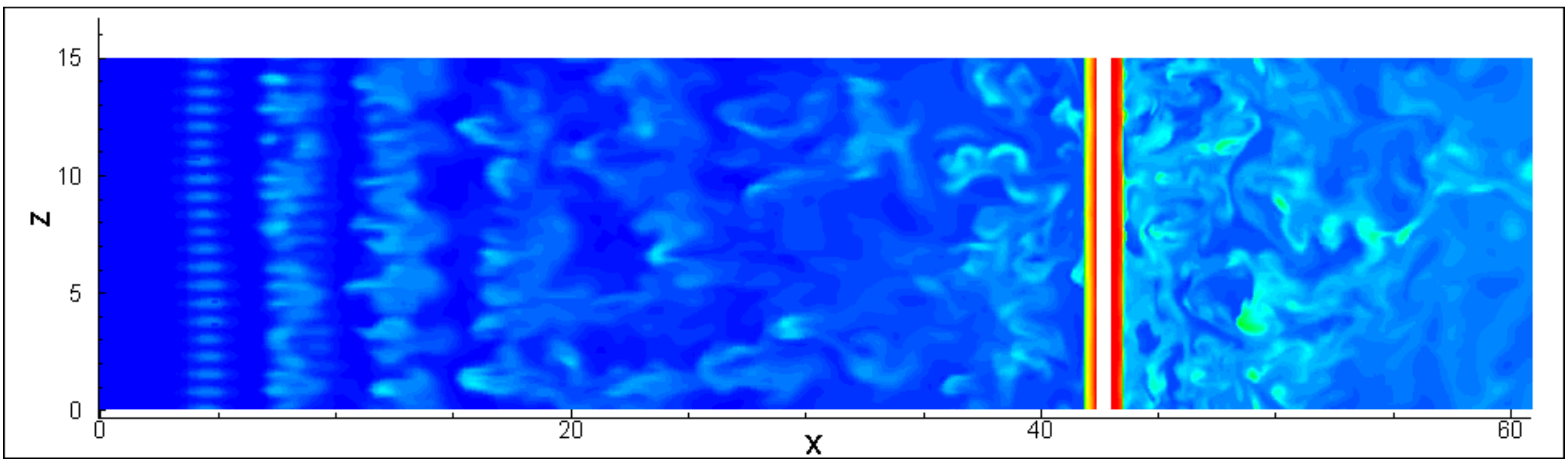

Heating starts at x=0 on the bottom plate. The BL is thermally unstable…

The Effect of Solid Conduction

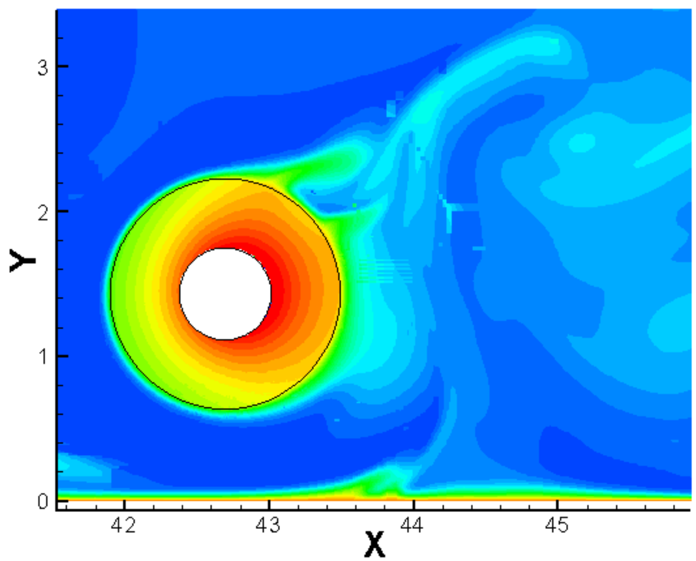

Highly unsteady turbulent flow field in the wake result in motion of the separation points on the cylinder

Thermal plumes from the upstream BL hit the cylinder at the stagnation point

As a result the wall temperature is NOT stationary

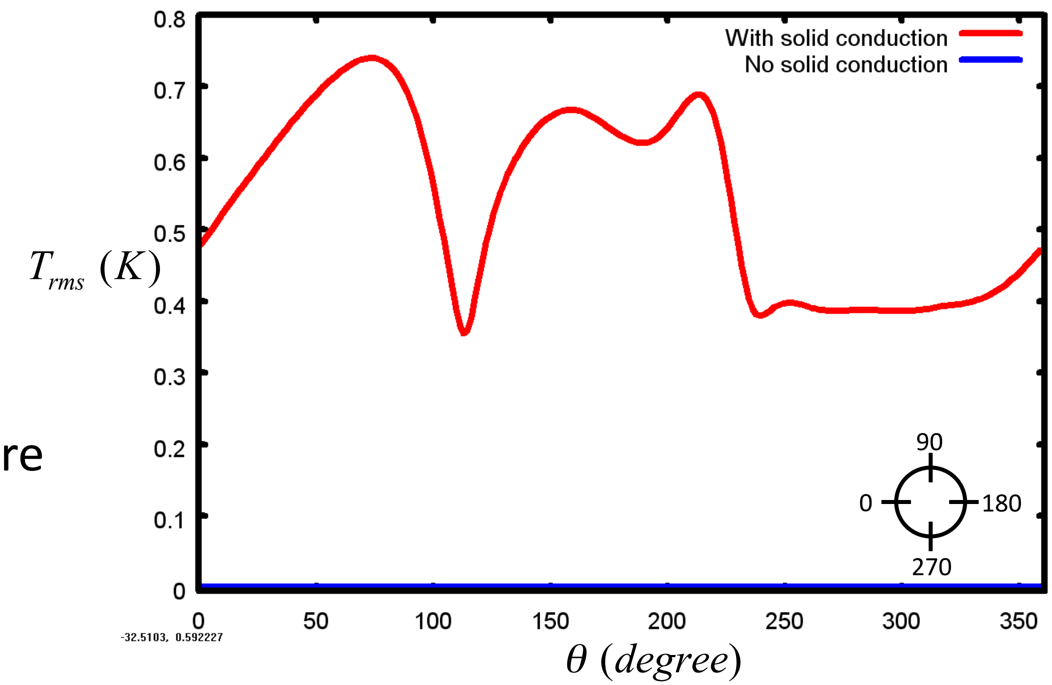

The Effect of Solid Conduction

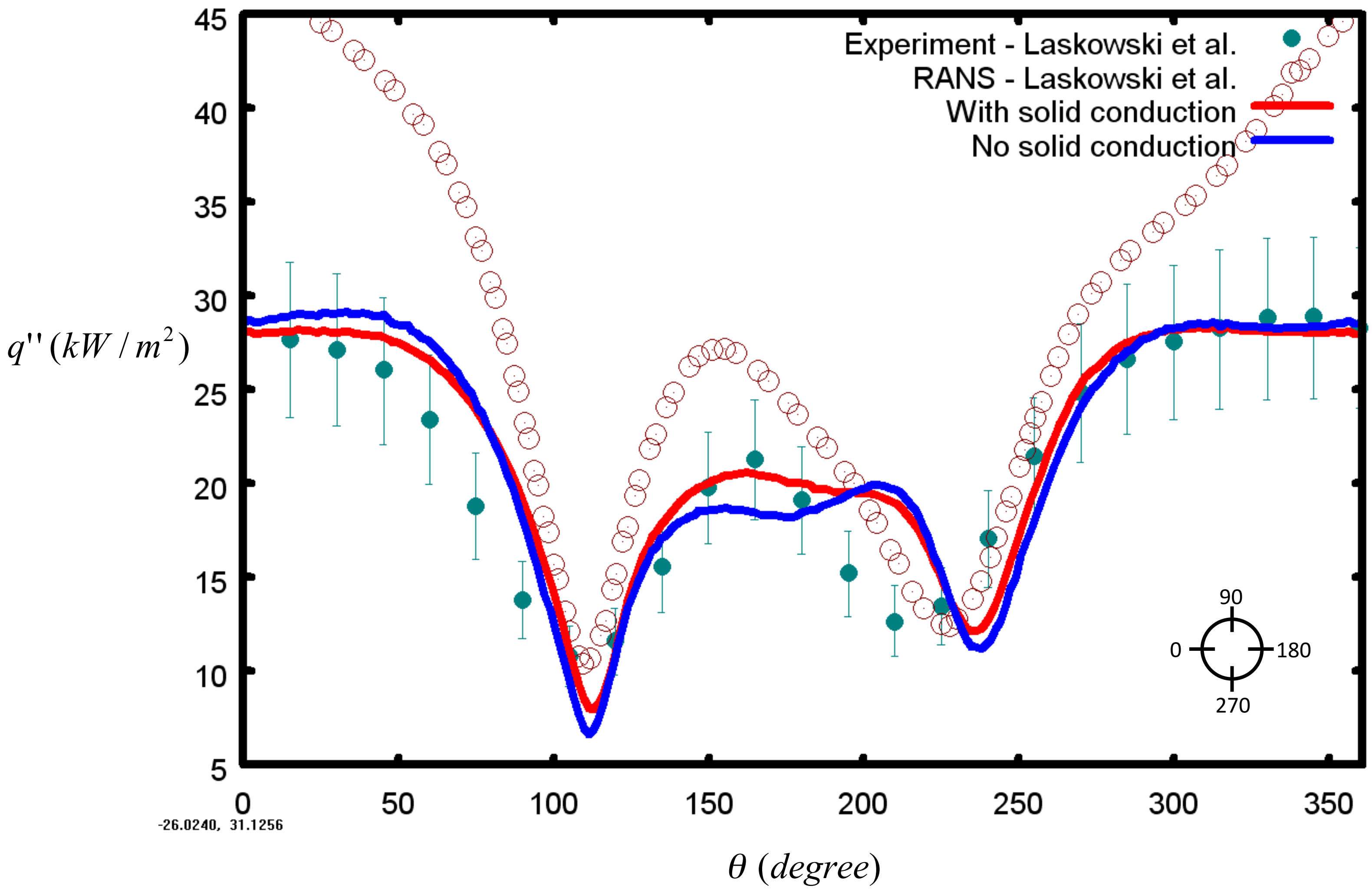

Instantaneous Temperature Field

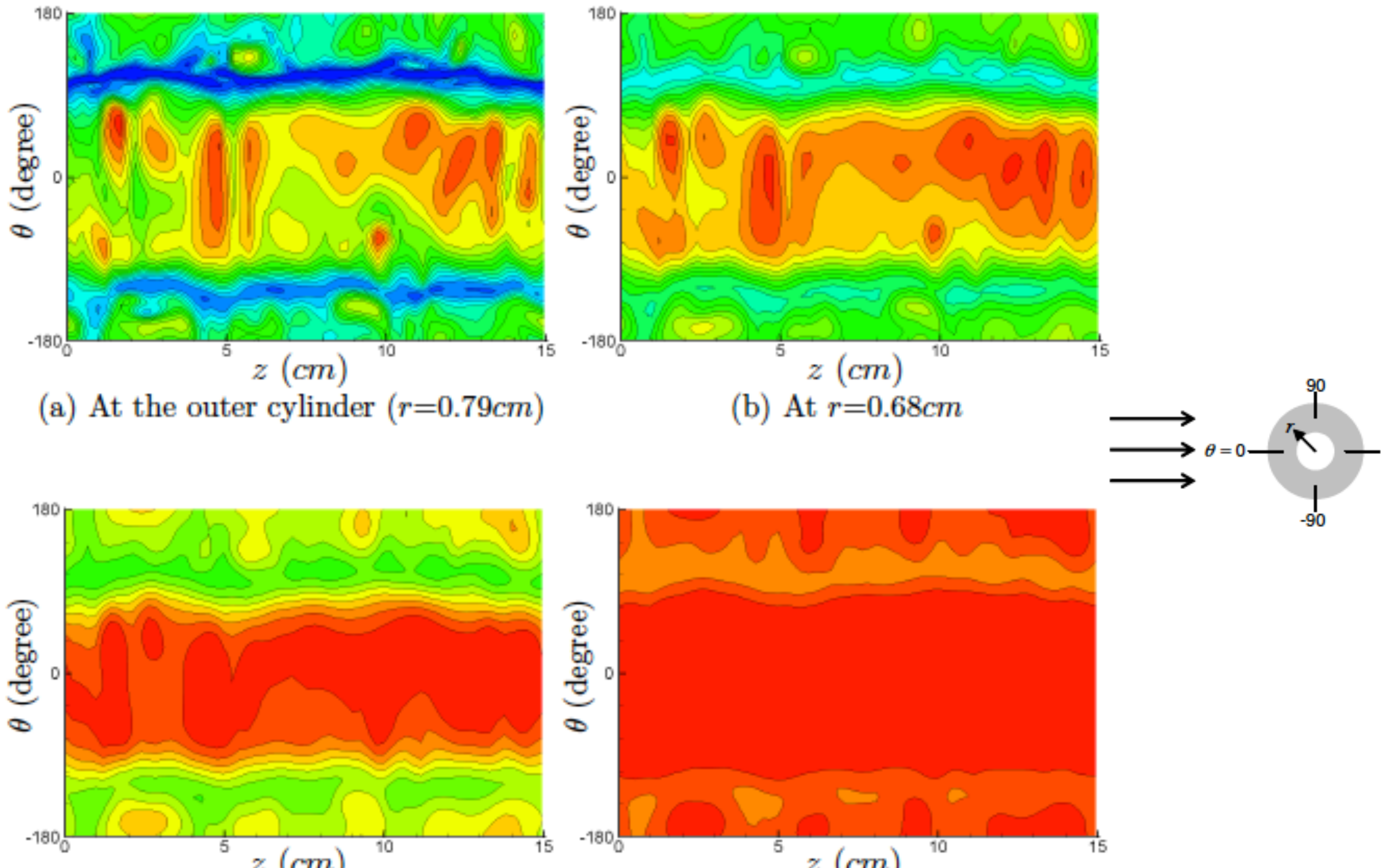

(a) At the outer cylinder (r=0.79cm)

(b) At r=0.68cm

(c) At r=0.57cm

(d) At r=0.47cm

6. Applications

Solid/Fluid Thermal Coupling
Using the Immersed Boundary Method

Electronic Component Units

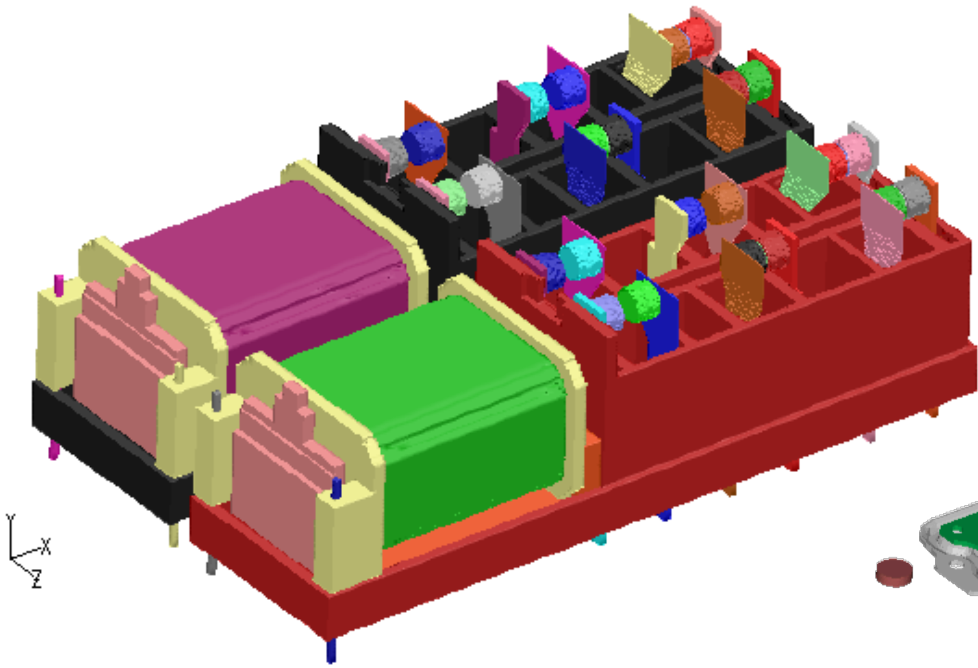

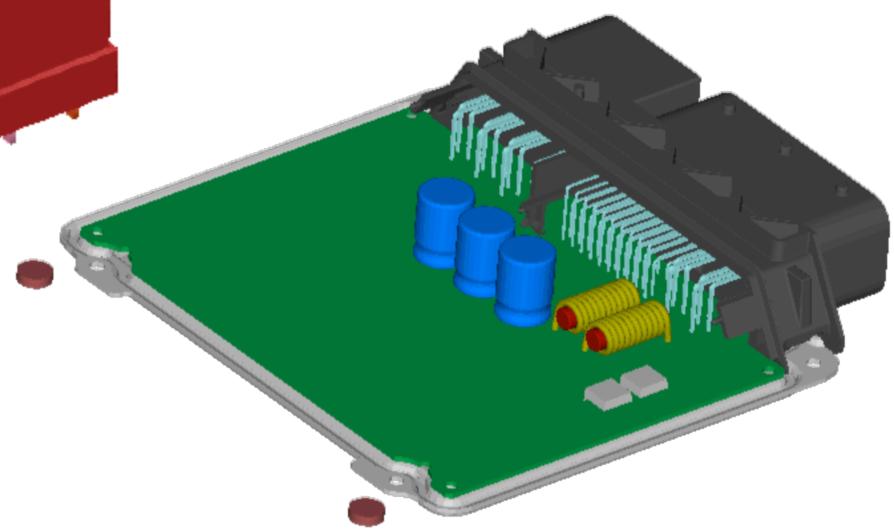

Electronic Components

A simple test case: Conduction + Natural Convection

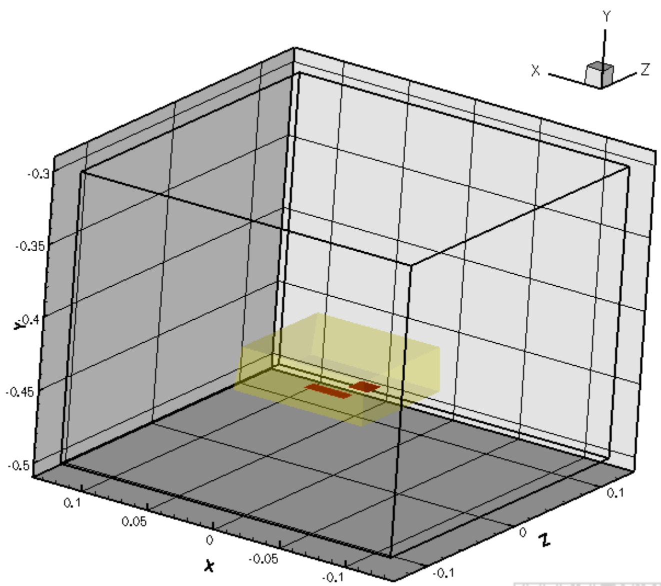

2 Hot Spots (CPUs)
1 Plastic Mold
in a air-filled cavity

Body-Fitted
420K Cells

IB
380K Cells

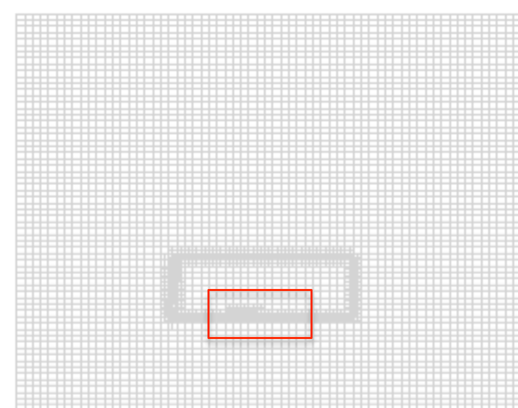

Electronic Components

A simple test case: Conduction + Natural Convection

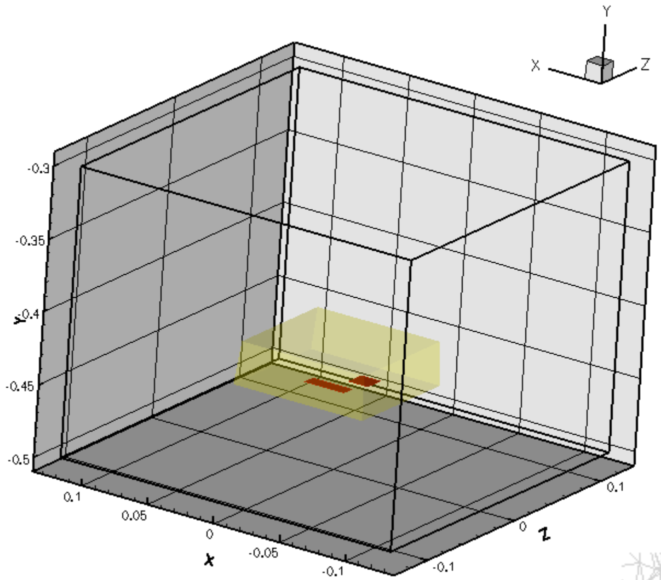

2 Hot Spots (CPUs)
1 Plastic Mold
in a air-filled cavity

Body-Fitted
420K Cells

IB
380K Cells

Temperature Field

Body Fitted

Immersed Boundary

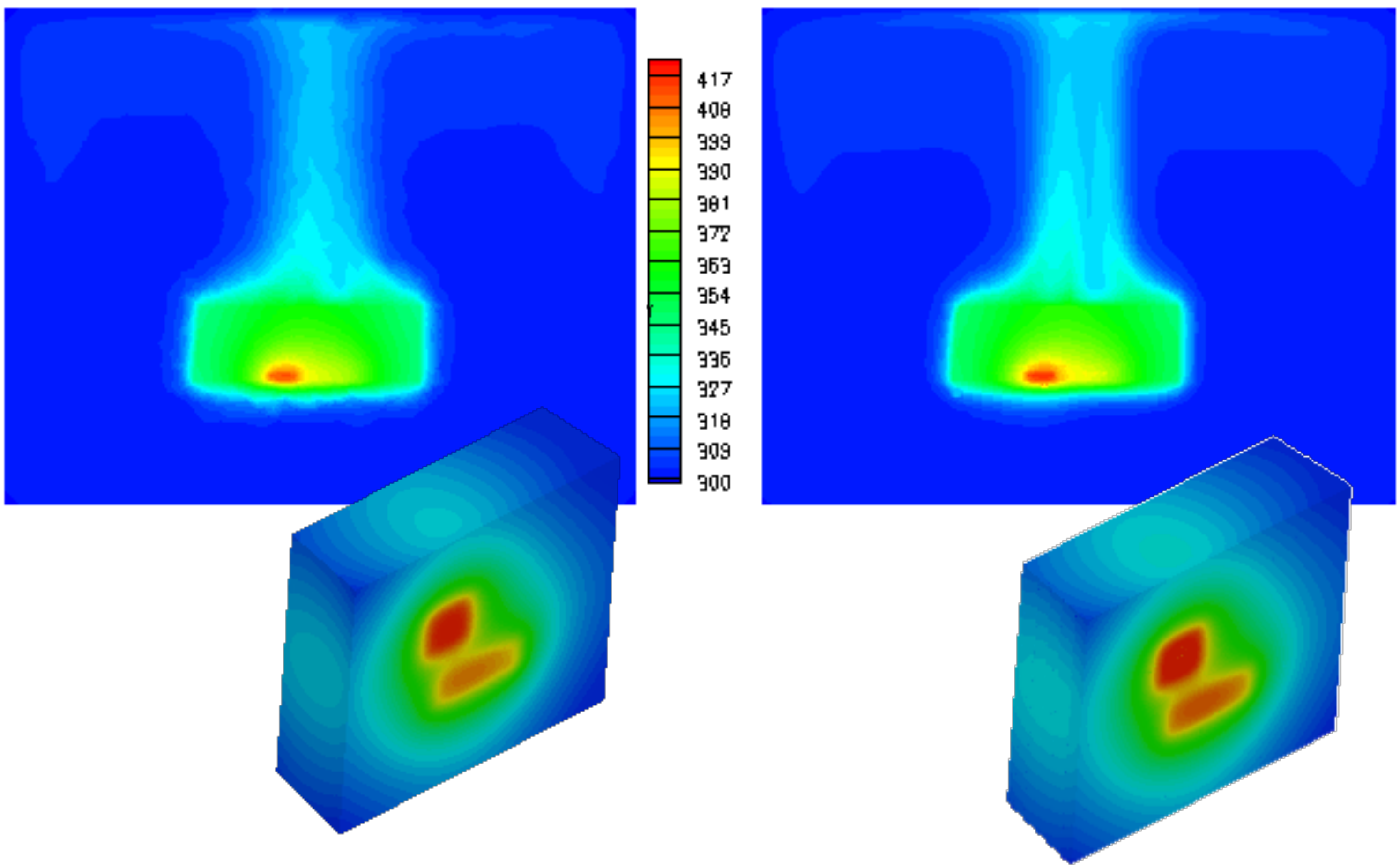

Velocity Field

Body Fitted

Immersed Boundary

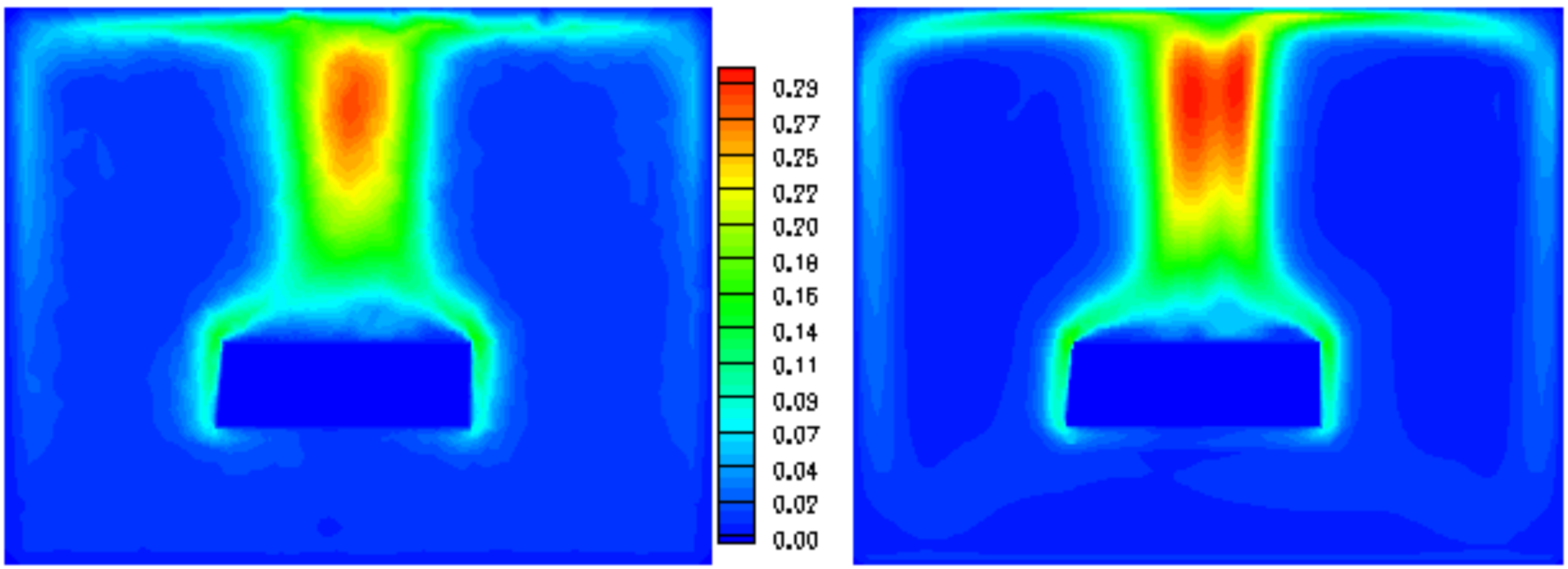

Electronic Component Unit

A complex test case: Conduction + Forced Convection

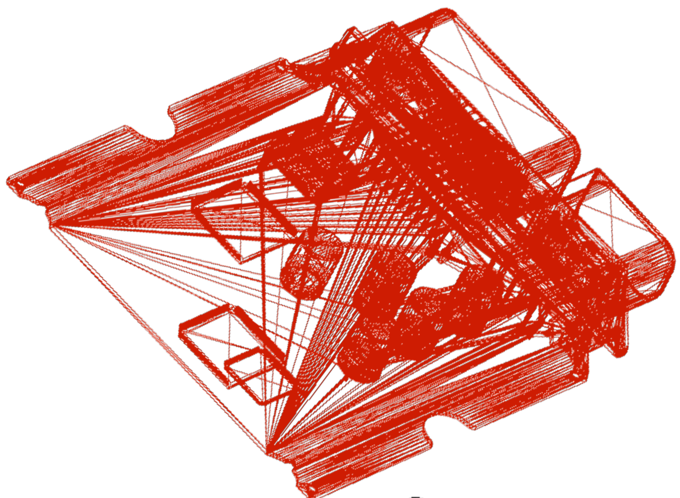

STL Geometry

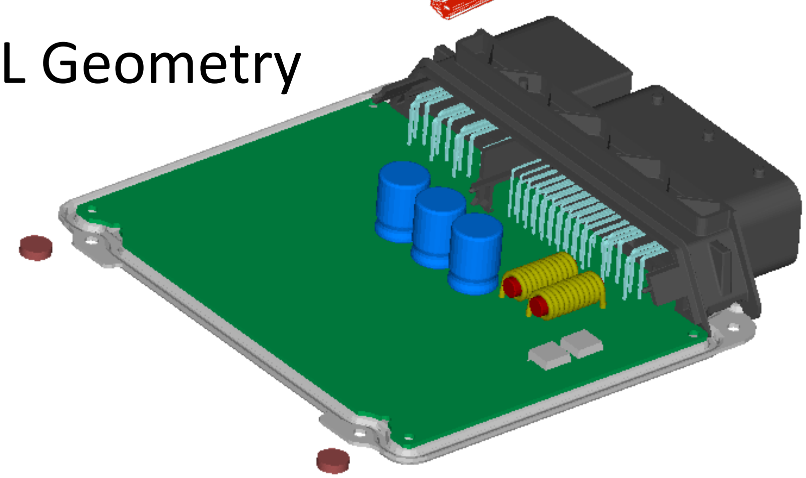

- Cartesian mesh
  - ~ 5.2 million cells
- Mesh contains ~10 solid zones for calculating conjugate heat transfer

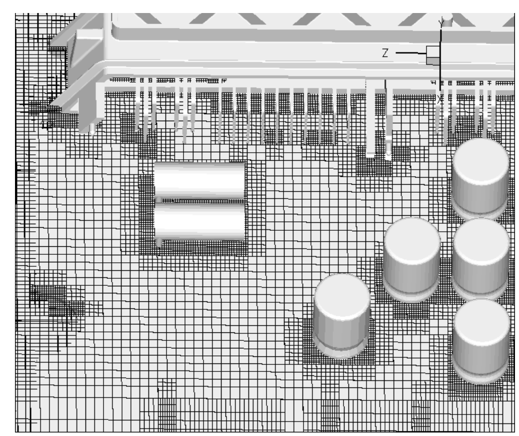

Electronic Component Unit

T_{top} | T_{bottom} | Velocity

CASE 1:
T_{max} = 322 K

CASE 2:
T_{max} = 325 K

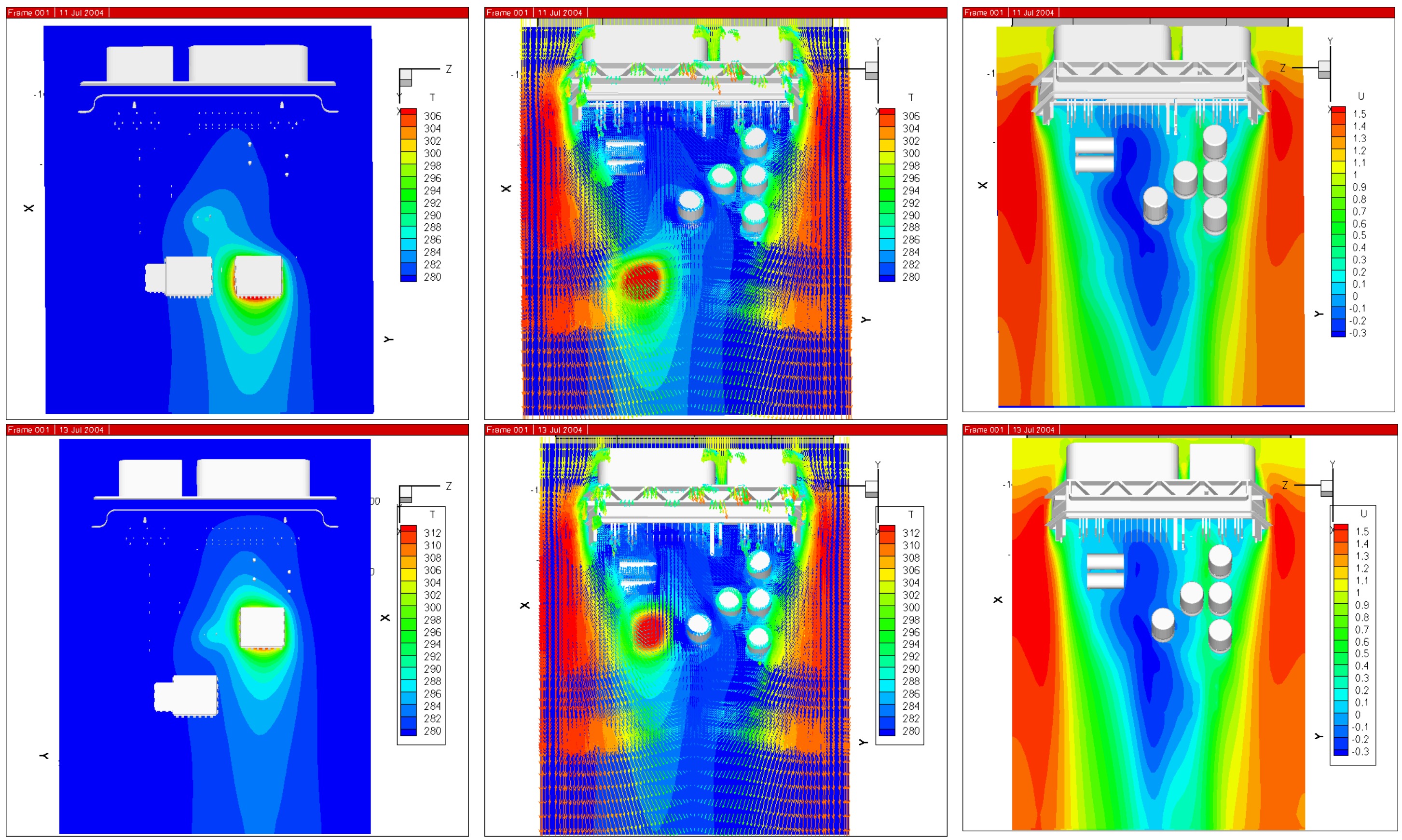

Electric Motors

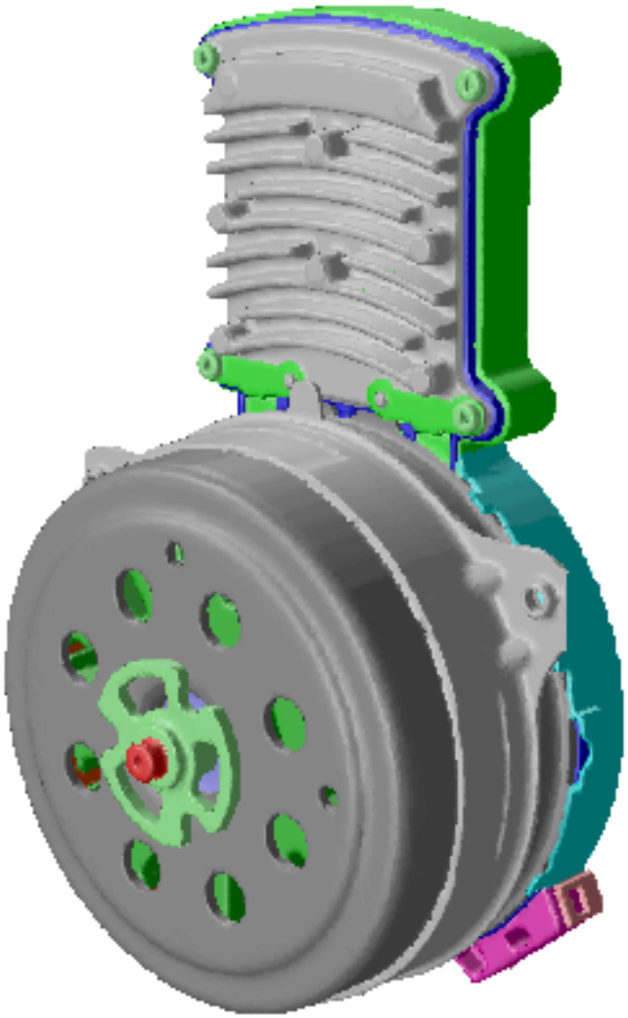

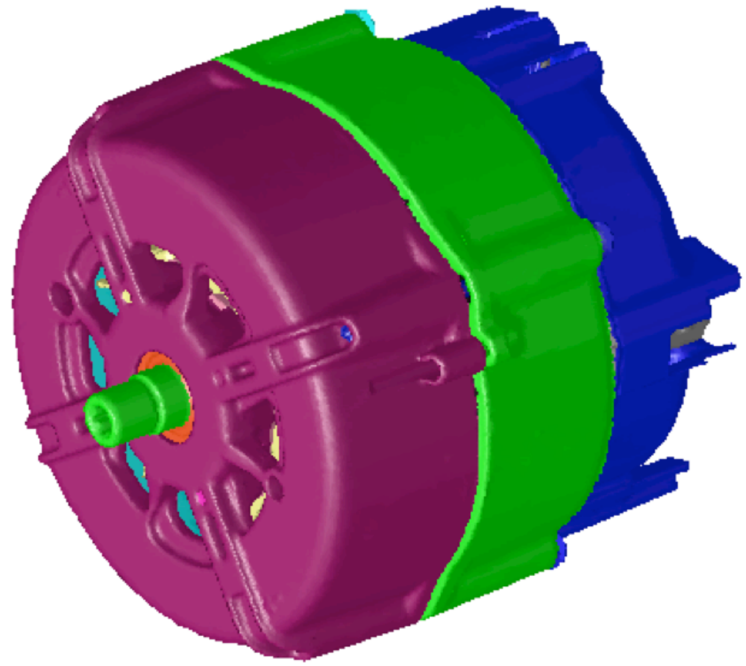

The "world" is NOT Cartesian

Many of the industrial applications have moving/rotating parts and Cartesian grids are not ideal

Example: Valeo Electric Motor

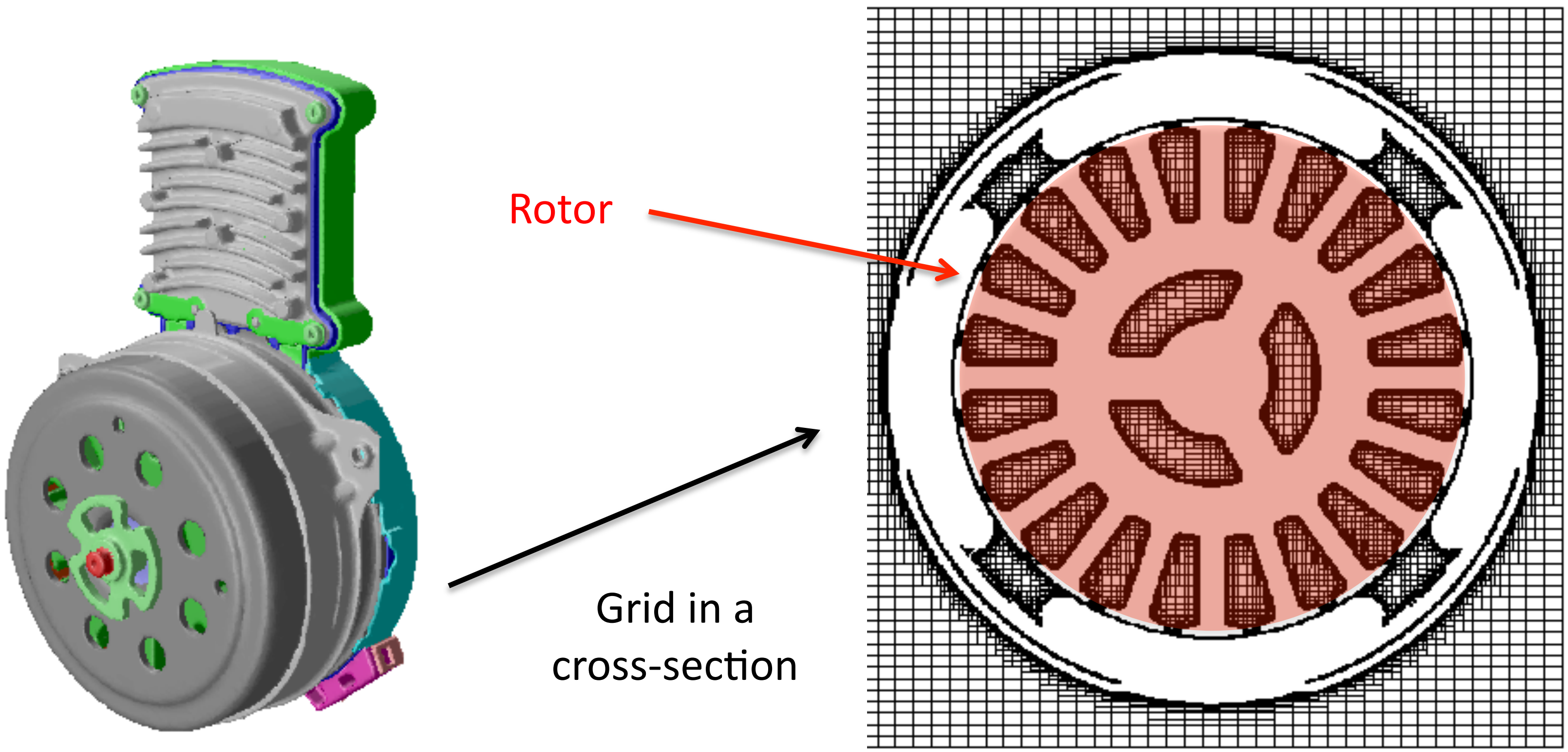

Beyond Cartesian Grids

The grids are not generated in the Physical Space but in a notional, integer space

- Addition of cells, and geometrical info are fast
- Tri-segment intersections are “exact”

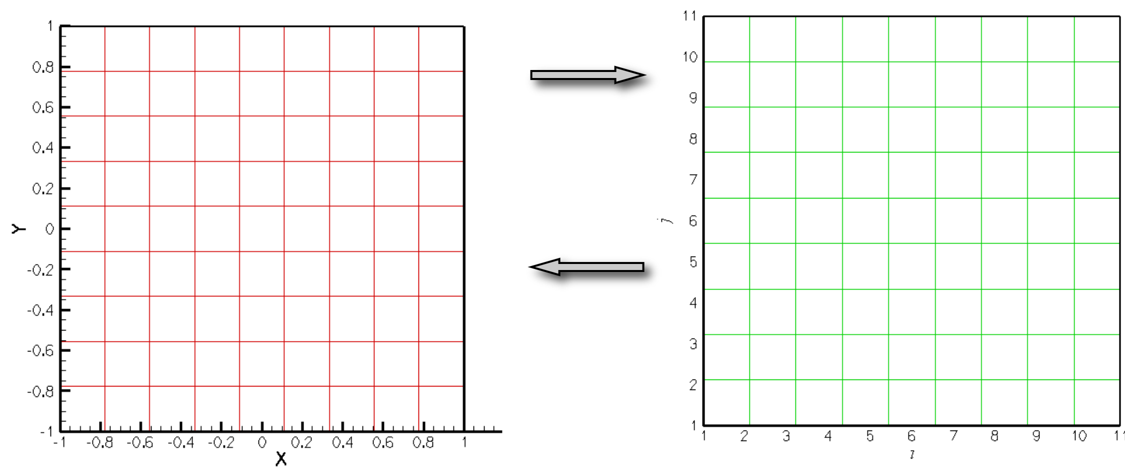

Physical Space
(Real X Real)

Notional Space
(Integer X Integer)

Beyond Cartesian Grids

A coordinate transformation can be applied to the entire process

- Cylindrical-to-Cartesian
- Any generic invertible transformation

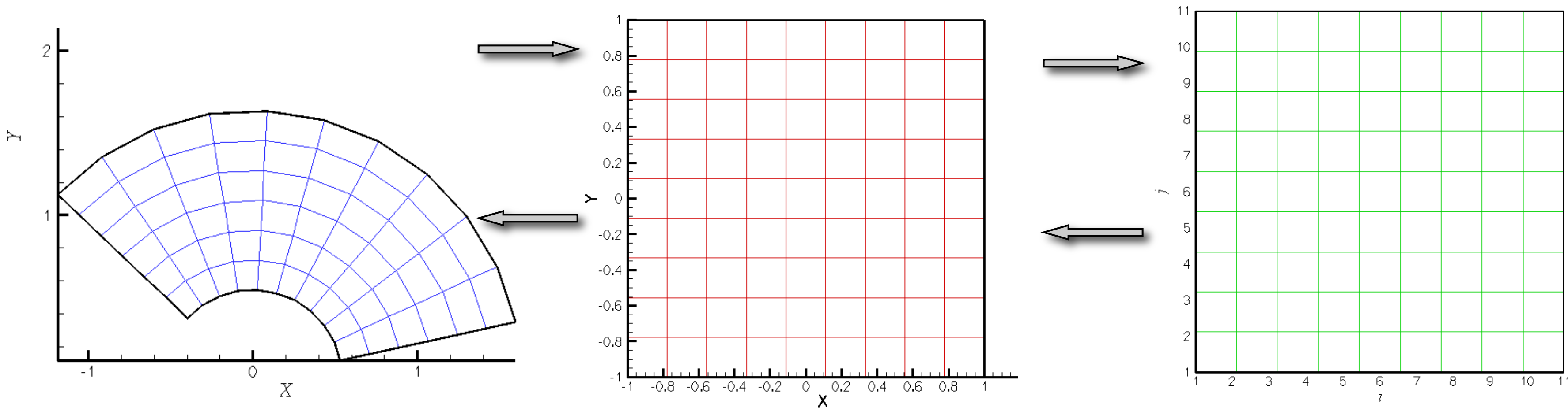

Physical Space
(Real X Real)

Transformed Space
(Real X Real)

Notional Space
(Integer X Integer)

From Cartesian to Cylindrical

Example: Valeo Electric Motor

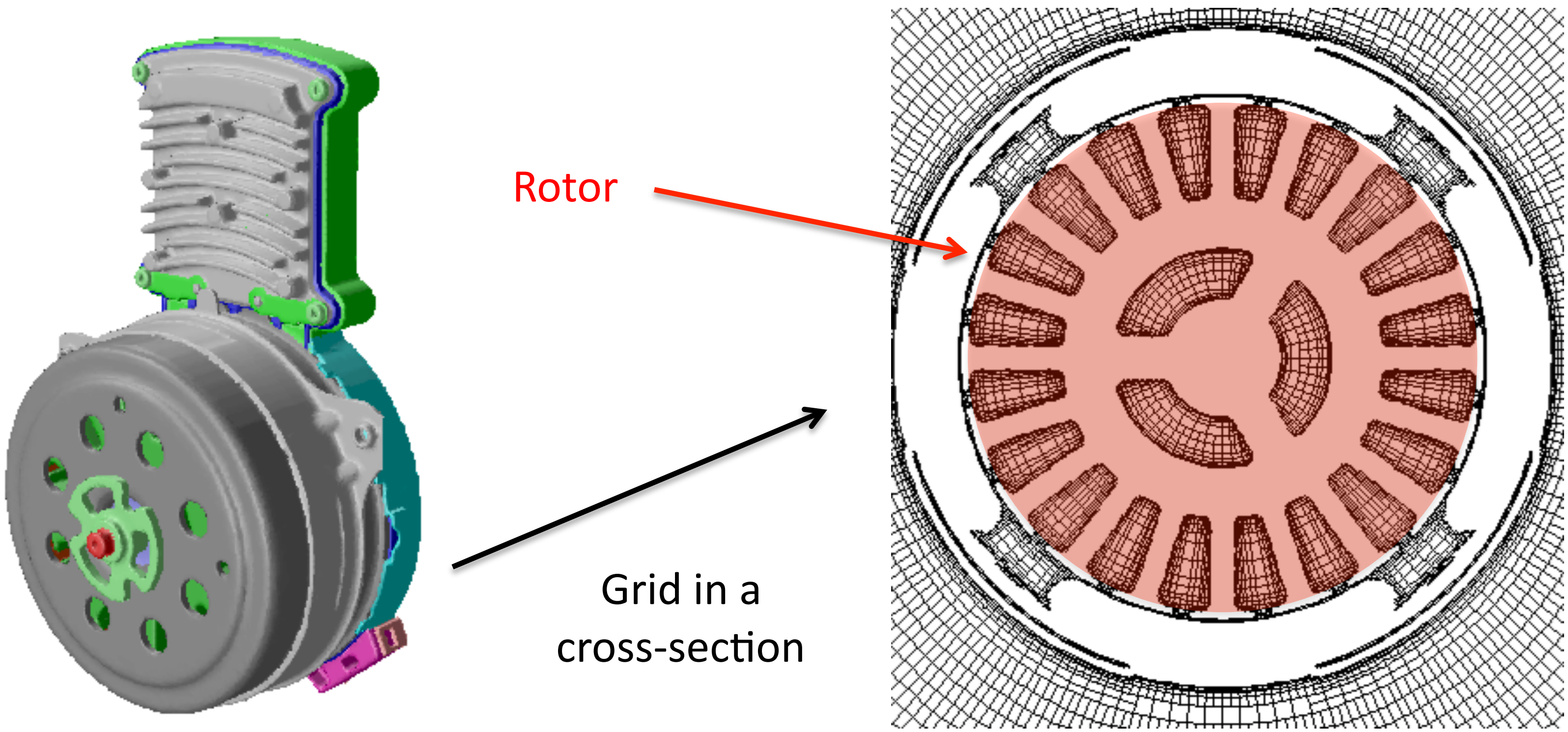

Alternator

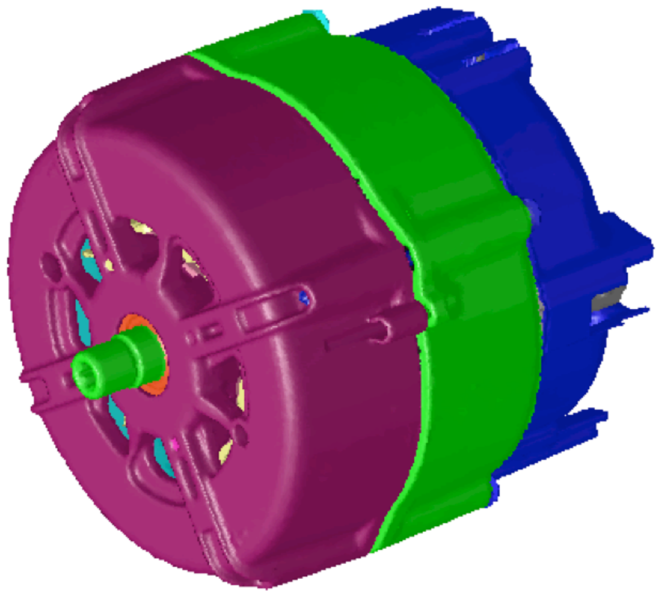

- Cylindrical mesh
  - ~ 16.2 million cells
- Mesh contains ~40 solid zones for calculating conjugate heat transfer

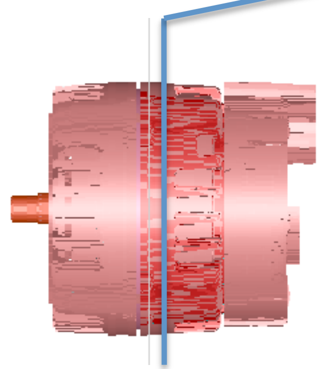

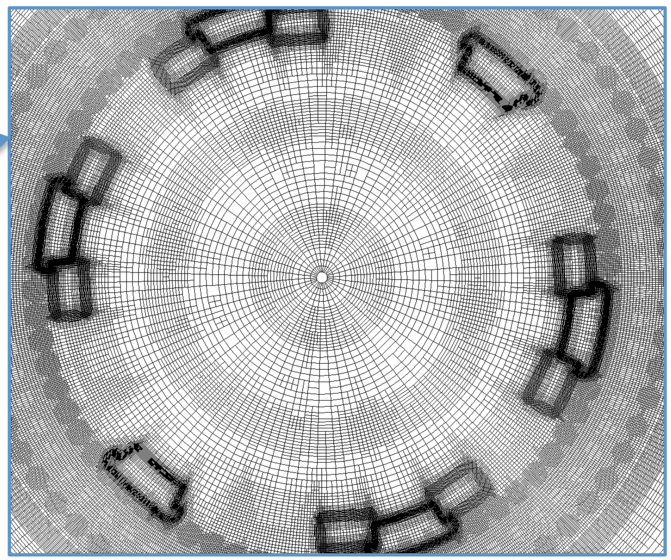

Alternator

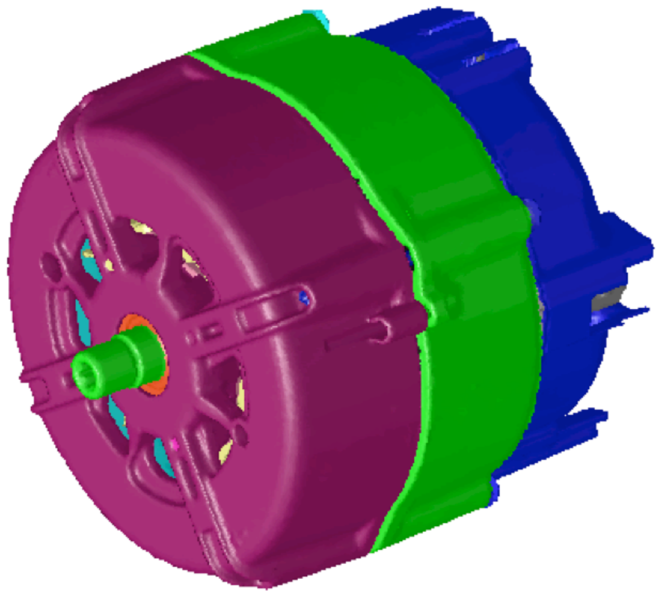

- Cylindrical mesh
  - ~ 16.2 million cells
- Mesh contains ~40 solid zones for calculating conjugate heat transfer

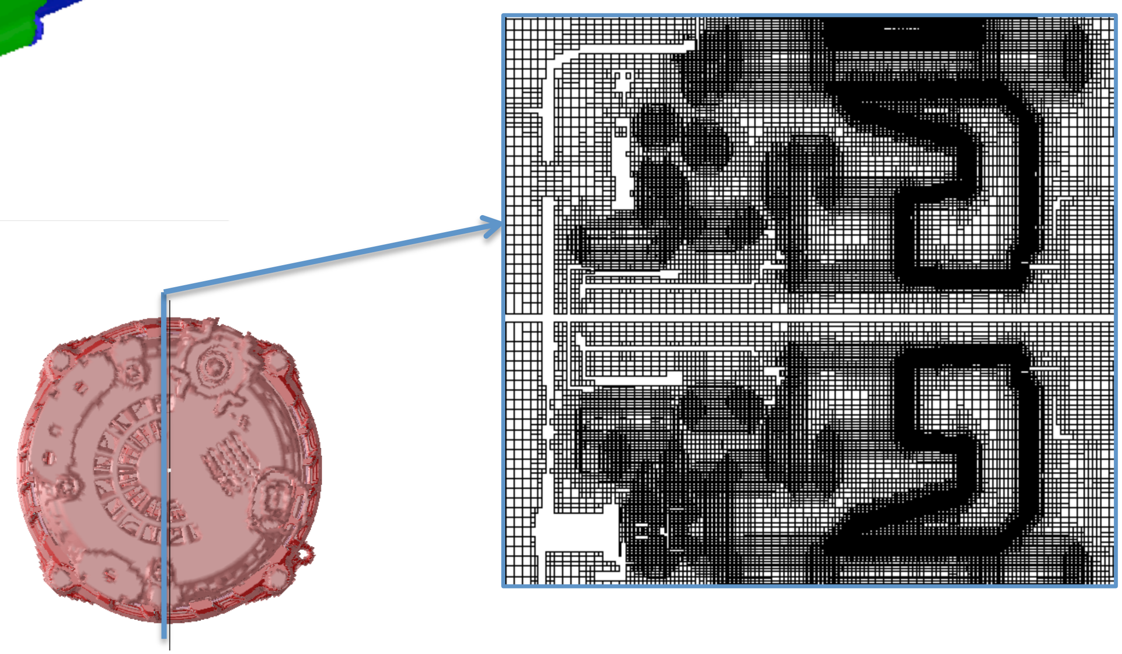

Alternator

Pressure

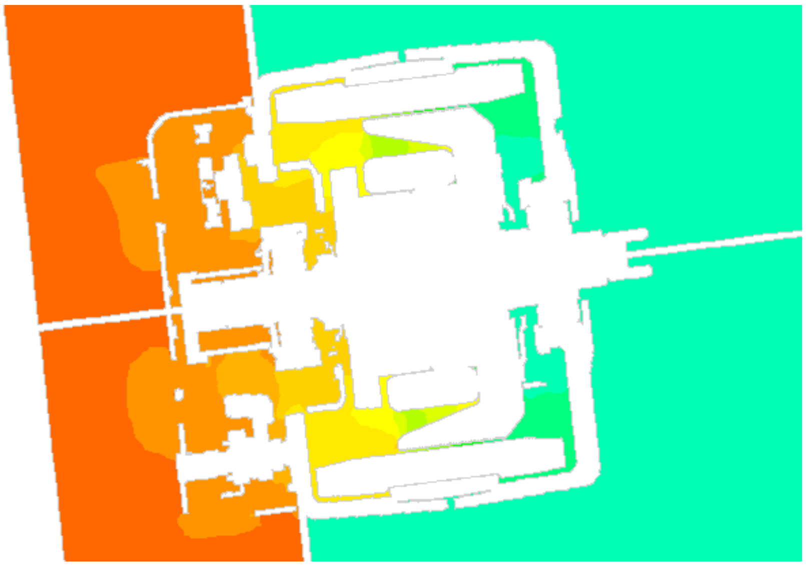

Velocity

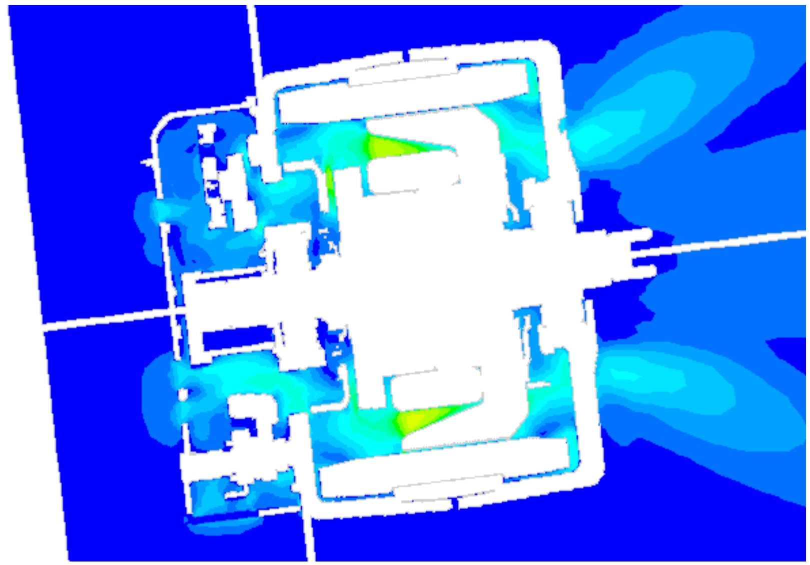

Flow Rate (CFM)	Pressure Drop (in. water)	
	Experiment	Simulation
2.0	0.075	0.087
3.0	0.11	0.13
5.0	0.195-0.225	0.247

Simulations vs. Experiments

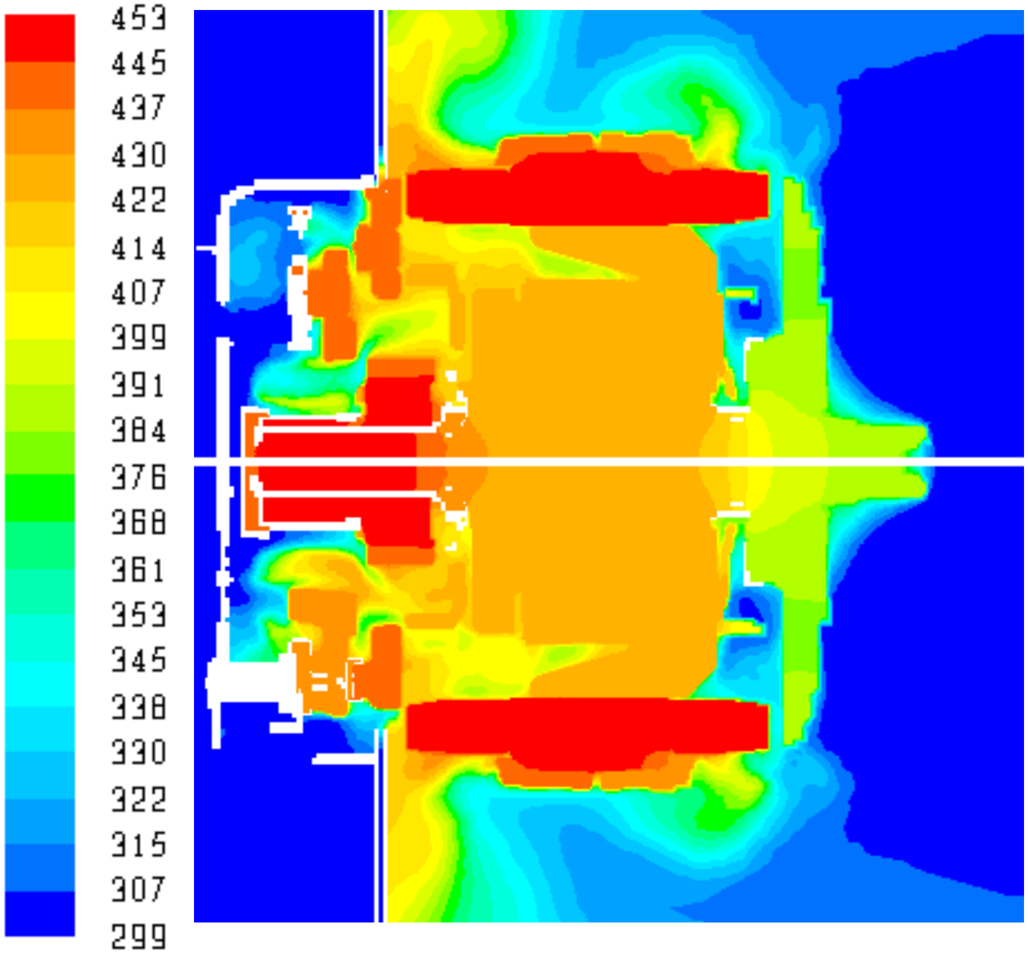

	Simulation	Test results
Stator copper	453	471
Stator iron	450	456
Front bearing	391	366
Rear bearing	450	389
diodes	440	418

Temperature

7. Closing

Solid/Fluid Thermal Coupling
Using the Immersed Boundary Method

Beyond CHT

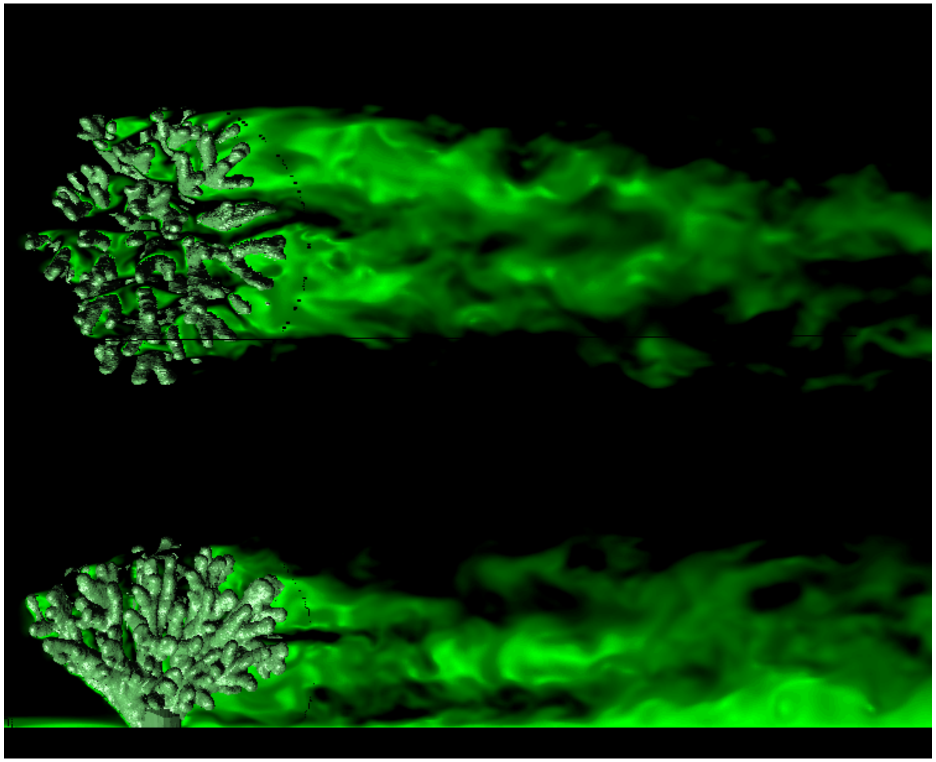

Nutrient Transport in Coral Reefs

Hazard Dispersion In Urban Environments

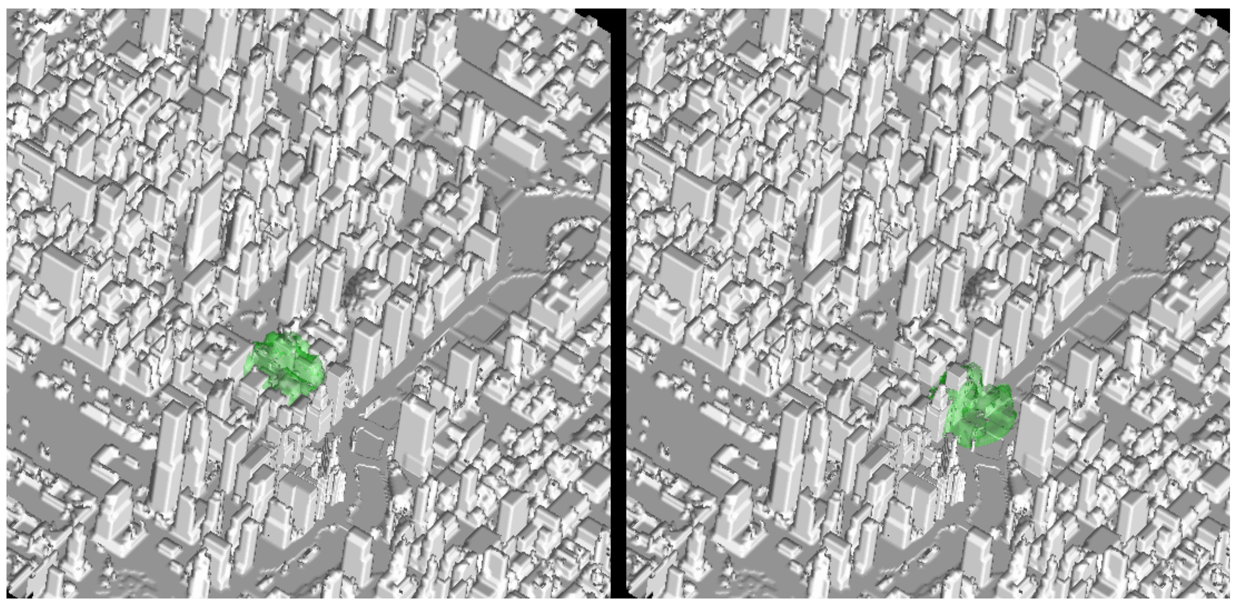

References

General Review: Mittal & Iaccarino, Ann. Rev. Fluid Mech. Vol. 37, pp. 239-261, 2005.

Review focused on turbulence: Iaccarino & Verzicco, Applied Mechanics Review, Vol. 56, No. 3, pp. 331-347, 2003.

IB for Incompressible LES: Verzicco, Fatica, Iaccarino, Orlandi, AIAA J. Vol. 40, pp. 177-191, 2002

IB for Compressible RANS: de Tullio, Iaccarino, et. Al. J. Comp. Physics, Vol. 225, pp. 2098¬2115, 2007.

IB Reconstructions: Kang, Moin, Iaccarino, AIAA J., Vol. 47, No. 7, pp. 1750-1760, 2009.

Local Mesh Refinement: Durbin, Iaccarino, J. Comp. Physics, Vol. 181, pp. 639,651, 2002.

IB Conjugate Heat Transfer: Kang, Ham, Iaccarino, J. Comp. Physics, Vol. 228, pp. 3189¬3208, 2009.

IB Heat Transfer: Iaccarino, Moreau, J. Fluids Eng., Vol. 128, pp. 838¬855, 2006.

Acknowledgements

Collaborators

R. Verzicco, F. Ham, M. de Tullio, S. Kang,
G. Kalitzin, S. Das, D. Cook

Funding

Valeo, Siemens, GM, Bosch

Also

The Organizer, WSC Conference

Thank You